

Optimal planning of robust DSO grid

Dissertation presented by
Quentin LÉTÉ

for obtaining the Master's degree in
Mathematical Engineering

Supervisors
Gauthier DE MAERE D'AERTRYCKE, Anthony PAPAVALIIOU

Readers
François GLINEUR, Yves SMEERS

Academic year 2017-2018

Acknowledgements

First of all, I would like to express my sincere gratitude to my supervisors, Anthony Papavasiliou and Gauthier de Maere.

I have to thank Anthony Papavasiliou for introducing me in such an inspiring way to the field of Energy Economics and Operations Research and for the passion that he was able to pass on during his lectures. I thank him for his commitment in the supervising of my master thesis and for his numerous comments, from the most fundamental to most detailed, that enabled me to keep improving this text.

I am very grateful to Gauthier de Maere for all the time he dedicated to the supervision of this work. I thank him for proposing the topic of this master thesis, for the enthusiasm in the topic he conveyed to me and for patiently sharing with me his understanding of optimization and the electricity market. I would also like to thank him for welcoming me at Engie's office all year long.

My thanks go to Pr. François Glineur and Pr. Yves Smeers for agreeing to be part of the jury of my master thesis.

My time at university was a demanding and captivating period of my life and I would like to thank all the people with whom I shared these five years, my classmates, my friends and my family. In particular, I would like to thank my parents for their unconditional support.

Disclaimer : “The views set out in this study are those of the author and do not necessarily reflect the opinion of ENGIE.”

Abstract

This master thesis proposes to model the robust planning of the DSO grid. The model includes the possibility for the DSO to invest in storage, reinforce its network and impose fuse limits which are limits on the reinjection and withdrawal of power in and from the network. The problem takes also into account the operational costs and determines the optimal power flow in the alternating current grid. A primal-dual algorithm is then used to find the optimal solution that is robust to uncertainties. The nonconvex optimal power flow equations are solved using an inexact second-order cone programming relaxation and a sequence of convex problems to recover the feasibility of the solution. Experiments are then performed on a real distribution network with large amount of renewable production and we demonstrate how our approach can help to reduce the curtailment of PV production.

Contents

Notations	vi
1 Introduction	1
1.1 Understanding the transition of the electric power system	1
1.2 The DSO at the core of the transition	2
1.3 Our contributions	4
2 Model	6
2.1 ACOPF constraints	6
2.1.1 Angle relaxation	8
2.1.2 SOCP relaxation	9
2.2 Fuse limits	9
2.3 Line reinforcement	12
2.4 Storage capacity investment	15
2.5 Optimal DSO planning	16
2.6 Robust formulation	18
2.6.1 Uncertainty set	18
3 Solution	22
3.1 ACOPF as a sequence of SOCP	22
3.2 Two-stage algorithm	27
3.2.1 First-stage solution	28
3.2.2 Second-stage solution	29
3.3 How to find C_f ?	29
3.4 Dual problem	30
3.4.1 Distribution Locational Marginal Prices	30
3.4.2 Dual of the complete problem	32
4 Results	38
4.1 Description of the dataset	38
4.1.1 Distribution grid	38
4.1.2 Residential load and generation	39
4.1.3 Battery storage modeling	39
4.1.4 Voltage control	40
4.1.5 Line reinforcement	40
4.1.6 Other parameters	40
4.2 Impact of Δ_1^{PV}	41
4.3 Impact of Δ^{EV}	44
4.4 Evolution of DERs	48
4.5 Analysis of robustness	50

4.5.1	Robustness on PV location	50
4.5.2	Location in the worst case	51
4.6	Gap of the Feasibility Recovery Procedure	52
4.7	Execution time and number of iterations	53
4.8	Conclusion to the real case analysis	54
5	Conclusion	55
A	Evolution of the power price in a path graph	59

Notations

Sets

\mathcal{N}	Set of nodes of the network.
\mathcal{N}_+	Set of nodes of the network except the substation node.
\mathcal{E}	Set of edges in the network.
\mathcal{T}	Set of time steps.
\mathcal{T}_+	Set of time steps except the first one.
\mathcal{T}_-	Set of time steps except the last one.
\mathcal{T}_d	Set of time steps that belong to day d .
\mathcal{C}_i	Set of children of node i .
\mathcal{G}	Set of choices for line reinforcement.
\mathcal{D}	Uncertainty set for the demanded injection.
$\tilde{\mathcal{D}}$	Extended uncertainty set for load, PV production and EV charge.
\mathcal{X}	Set of constraints containing only first-stage variables.
\mathcal{Y}	Set of constraints containing second-stage variables.
$\mathcal{Y}_{\text{SOCP}}$	Set \mathcal{Y} where the nonconvex quadratic constraint has been relaxed to the corresponding convex inequality.
\mathcal{Z}_k	Feasible set for the variables used in the FRP.
\mathcal{S}	Set of worst-case candidates.
\mathcal{K}	Cone corresponding to set \mathcal{Z}_k .

Variables

$v_{i,t}$	Square of the norm of the complex voltage at node i and time t .
$p_{i,t}$	Active power injection at node i and time t .
$q_{i,t}$	Reactive power injection at node i and time t .
$l_{i,t}$	Square of the norm of the complex current of line i and time t .
$P_{i,t}$	Real power flow in line i and time t .
$Q_{i,t}$	Reactive power flow in line i and time t .
$\tilde{l}_{i,t,g}$	Square of the norm of the complex current of line i and time t if choice g is made, 0 otherwise.
$\tilde{P}_{i,t,g}$	Active power flow on line i and time t if choice g is made, 0 otherwise.
$\tilde{Q}_{i,t,g}$	Reactive power flow on line i and time t if choice g is made, 0 otherwise.
\bar{K}, \underline{K}	Upper and lower fuse limits.
$x_{i,t}^+$	Curtailement performed at node i and time t due to overproduction.
$x_{i,t}^-$	Curtailement performed at node i and time t due to overconsumption.
w_g	Binary variable indicating the choice made.
$e_{i,t}$	Energy stored in the battery at node i and time t .
f_i	Storage investment at node i .

$p_{i,t}^{in}$	Active power input to be stored at node i and time t .
$p_{i,t}^{out}$	Active power output to be stored at node i and time t .
u_i^{PV}	Uncertain binary parameter indicating whether there are PV panels at node i .
$d_{i,t}^{PV}$	Uncertain parameter corresponding to the PV production at node i and time t .
u_i^{EV}	Uncertain binary parameter indicating whether there is an EV at node i .
$d_{i,t}^{EV}$	Uncertain parameter corresponding to the EV consumption at node i and time t .
$s_{j,t}$	Slack variable penalizing the SOCP gap in the objective.

Parameters

A_i	Ancestor of node i .
$d_{i,t}$	Active net power injection demanded at node i and time t .
z_i	Complex impedance of line i .
r_i	Resistance of line i .
x_i	Reactance of line i .
\bar{L}_i	Length of line i .
r_g	Resistance of all lines in choice g .
x_g	Reactance of all lines in choice g .
I_g	Current capacity limit of all lines in choice g .
C_l	Cost of losses.
C_f	Cost of fuse.
C_+	Cost of curtailment due to overproduction.
C_g	Cost of reinforcement in choice g .
\mathbb{L}^n	n^{th} order Lorentz cone.
x^{planned}	Planned curtailment.
$x^{\text{unplanned}}$	Unplanned curtailment.
$x_{\text{unplanned}}^{\%}$	Percentage of unplanned curtailment.
\bar{P}, \underline{P}	Upper and lower bound on the active power flow.
\bar{Q}, \underline{Q}	Upper and lower bound on the reactive power flow.
$\underline{p}_i^{in}, \overline{p}_i^{in}$	Lower and upper bound on the active power input at node i .
$\underline{p}_i^{out}, \overline{p}_i^{out}$	Lower and upper bound on the active power output at node i .
h	Duration of a time step.
ξ_{in}, ξ_{out}	Charging and discharging battery factors.
Δ_1^{PV}	Budget parameter on the number of PV installations.
Δ_2^{PV}	Budget parameter on the uncertain PV production.
C	EV batteries storage capacity.
Δ^{Load}	Budget parameter on the uncertain load.
ρ^1	Initial penalty parameter of FRP.
τ	Penalty growth rate parameter.
ρ_M	Penalty upper bound.
ϵ	Feasibility tolerance of the nonconvex constraint.

Acronyms

ACOPF Alternating Current Optimal Power Flow.

ADMM Alternating Directions Method of Multipliers.

CCP Convex-Concave Procedure.

DCOPF Direct Current Optimal Power Flow.

DER Distributed Energy Resources.

DSO Distribution System Operator.

EV Electrical Vehicle.

FRP Feasibility Recovery Procedure.

ICT Information and Communication Technologies.

LMP Locational Marginal Prices.

LP Linear Program.

MISOCP Mixed-Integer Second Order Cone Program.

ODP Optimal DSO Planning.

OPF Optimal Power Flow.

SOC Second Order Cone.

SOCP Second Order Cone Program.

VOLL Value Of Lost Load.

Chapter 1

Introduction

1.1 Understanding the transition of the electric power system

Indisputably, the electric power system is facing a huge transition. Understanding the fundamental reasons for this change is essential to develop new tools for decision making in the field. Based on [1], I will highlight the main ways in which the system is transitioning and the reasons for this transition.

How is the system changing ?

We can point out three main ways in which the system is changing. It is becoming :

1. More distributed. The past years have seen a rise of the number of Distributed Energy Resources (DER) available in the distribution networks. Examples of DER are renewable production at the distribution level, storage capacity, demand response, control devices, ...
2. Increasingly digitized. Information and Communication Technologies (ICT) are currently being increasingly deployed in the distribution grid to enable active real-time control and operation of the grid. Examples of these technologies include smart meters that are able to communicate with each other and with central operators.
3. Renewable and intermittent. The share of renewable energy in the power production increased dramatically in the last decade in many big countries and especially in Europe [2]. As a consequence, the production is much more intermittent and operators have to find new ways for dealing with this uncertainty.

Why is it changing ?

It is also interesting to investigate why this transition is happening now. The MITEI report ([1]) highlights here three main points :

1. Technological innovations. This implied huge cost decreases in many key technologies in electricity systems (LEDs, PVs, Batteries, ...).
2. Policies. Many policies related to the investment in renewable energy were adopted, with the goal of decarbonizing the energy system. This in part enabled the technological innovations mentioned above.

- Consumer choices. Some consumers choose to invest in renewable energy and environment friendly technologies per choice rather than per economic opportunity. This also participates to the positive investment climate around technologies for a more distributed, digitized and renewable energy system.

1.2 The DSO at the core of the transition

The electric power system is a large system with many actors. With the changes that this industry is facing, one agent will be particularly at the center of the transition : the Distribution System Operator (DSO). Let us in this section describe the role of the DSO for the time being and how its role is expected to evolve in the future.

The DSO is the company responsible for building, maintaining and operating the distribution network. It delivers electricity from the Transmission Grid or local producers to consumers, either residential or small factories. For the time being, the DSO plays a rather passive role in the operations of its electricity grid. In the past, very few electricity services were provided at the distribution level. The role of the DSO was thus to ensure that the electricity was delivered in a safe and reliable way to the consumers through its network. Its main means of action was to build new or bigger lines if the forecast indicated that the network could become saturated. The network was reinforced according to peak demand so that no constraints would be violated in real-time. This way of planning the network is often called a fit-and-forget approach. The MITEL report ([1]) states that it was an efficient and cost-effective way of managing the network in a centralized system but shows how it can become inefficient with the rise of DERs.

The following figure (Figure 1.1) represents schematically the role of the DSO and its means to plan and operate its network.

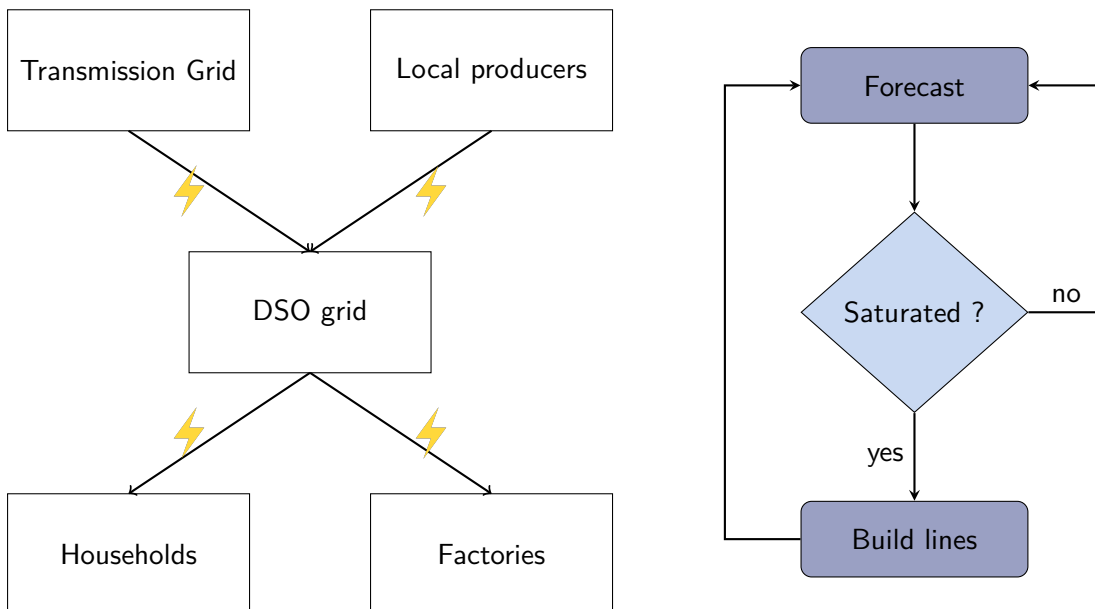


Figure 1.1: Role of the DSO at this time. Left : Flow of electricity in in the DSO network. Right : DSO planning and operation process.

With the advent of distributed production and other DERs in the distribution network, the role of the DSO is expected to change dramatically in the next decade. To highlight this point, I would like to refer again to the MITEL report :

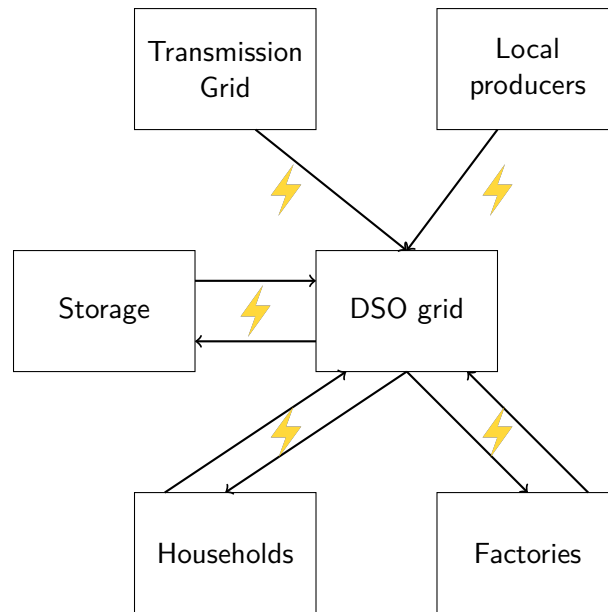


Figure 1.2: Role of the DSO in the near future : flow of electricity in in the network.

Distribution companies will have to become true “system operators”.

They argue that this will necessarily imply coupling operation and planning. In this work, we wish to develop a decision-making framework for the DSO to decide on the optimal way of planning and operating the distribution network with respect to the three following decisions :

1. Line reinforcement. The DSO can decide the specifications of the lines it will use in its network (resistance, reactance, maximum current).
2. Fuse limits. The DSO can impose limits on the consumption and production of power on its network.
3. Storage investment. The DSO can invest in storage facilities at each node of the network.

These decisions have to be made while respecting a set of constraints :

1. Physical laws. These includes Kirchhoff’s laws, voltage deviation constraints and current limit.
2. Robustness. The optimal decision has to be robust to the worst case realization of uncertainty. That is, it is not acceptable to violate voltage constraints or to fail to match the demand even in the worst case.
3. Computational tractability. It should be possible to find the optimal solution in reasonable time even for large, real-case instances.

Each of these decisions and constraints will be discussed in chapter 2 dedicated to the presentation of our model.

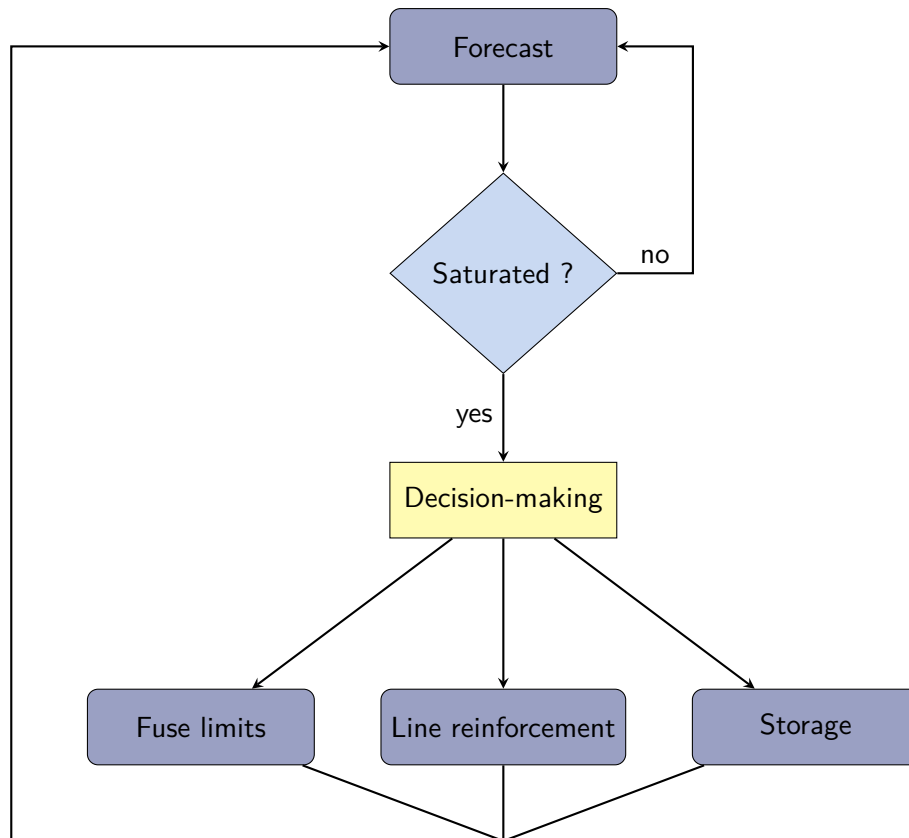


Figure 1.3: Role of the DSO in the near future : planning and operation process.

1.3 Our contributions

In this master thesis, we will use existing models and algorithms and combine them with new modeling features and methods to solve the problem of optimal planning and operation of distribution networks with large amount of DER. Our main contributions, both technical and in modeling, are the following :

Modeling

1. We model fuse limits as decisions that the DSO can make in the operations of its network and propose an original method to find them in an optimal way.
2. We propose a method for line reinforcement modeling.
3. Based on existing work on robust optimization with budget uncertainty sets ([3]), we propose an uncertainty set that is robust both to location of PV installations in the DSO network and to production profiles uncertainty.
4. We propose an uncertainty set for Electrical Vehicle location and charge timing.

Technical

5. We combine existing work on robust solution to the SOCP relaxation of the OPF ([4]) and on optimal solution to the non-relaxed problem ([5]) to solve the problem of optimal planning of DSO grid in a robust way.
6. We use the convex relaxation of the AC-OPF equations developed in [6] and [7] to derive a new formula for the evolution of the electricity price in a radial distribution network.

The present report is organized as follows :

In chapter 2, we present our model. We first sequentially present the ACOPF equations, the fuse limits, line reinforcement and storage models before combining them into the unified Optimal DSO Planning (ODP) model. We finish this chapter by the uncertainty sets modeling.

In chapter 3, we present the algorithms that enables us to solve the Optimal DSO Planning (ODP) in a robust way. In particular, we first present the feasibility recovery of the SOCP relaxation of the ACOPF. Then, the two-stage algorithm for solving the SOCP problem in a robust way is described. We also present our method for finding the optimal value of the fuse limits. We end this chapter by deriving the dual of the problem and discuss the interpretation of the dual variables of the SOCP.

Chapter 4 studies in depth the behavior of our decision framework for the DSO in the context of a real distribution network with realistic load and generation profiles. We first analyze the influence of the number of PV installations and EVs on the optimal solution. We then discuss the advantages of having a robust solution by highlighting the difference with a nonrobust solution before analyzing the performances of our algorithm.

Finally, chapter 5 proposes a conclusion to this master thesis and exposes the perspectives of further research.

Chapter 2

Model

This section aims to develop the optimization program used to model the planning of the DSO grid.

The DSO of the future will have the possibility to use the three following decisions :

1. Impose fuse limits on the injection and consumption of power at each node.
2. Choose the characteristics of the lines in the network.
3. Invest in storage.

The main constraints with which it is confronted are the constraints of the AC-OPF. In what follows we sequentially present and develop each of these elements to obtain the full model.

2.1 ACOPF constraints

The Optimal Power Flow (OPF) problem consists in finding the flow of power in an electrical network that minimizes losses or costs subject to the physical laws governing this flow. It has been widely studied in the literature and is one of the most important problems of power systems. There are different ways of formulating the OPF problem. The two main formulations are the bus injection model and the branch flow model. The bus injection model focuses on nodal variables whereas the branch flow model uses the value of currents and voltages on the branches of the network. In this work, we will use the branch flow model as it was shown in [6] and [7] that it exhibits good performances on distribution networks.

In addition to the constraints due to Kirchhoff's law, bounds on voltages and currents need also to be taken into account. The bounds on the voltage represent the acceptable deviation from the nominal value. The upper bound on the current represents the maximum value that the line can carry. The lower bound on the current imposes positivity.

The electrical network can be mathematically modeled as a graph whose edges represent the electrical lines and whose nodes are locations in the network where power can be consumed or injected. In a typical distribution network, the nodes correspond to households or small factories that behave as prosumers. In this work, we will make the assumption that the graph is a tree as it is the case of most distribution networks. Let \mathcal{N} be the set of nodes and \mathcal{E} be the set of edges.

We represent every node by an integer in $\{0, \dots, n\}$ where $n = |\mathcal{N}| - 1$, $|\mathcal{N}|$ being the cardinality of set \mathcal{N} . The root of the tree is the node that connects the distribution network to the transmission

network and is the node 0 in our model. We denote by \mathcal{N}_+ the set of nodes except the substation node, i.e. $\mathcal{N}_+ = \mathcal{N} \setminus \{0\}$. Each node $i \in \mathcal{N}_+$ has a unique ancestor denoted by A_i and each node $i \in \mathcal{N}$ has a set of children denoted by \mathcal{C}_i . We choose the orientation of the lines from being from i to A_i so that we can unambiguously represent each line by its origin node. We thus have $\mathcal{E} = \{1, \dots, n\}$. Therefore, the set \mathcal{E} is exactly the same as the set \mathcal{N}_+ . In what follows, we will only use \mathcal{N}_+ to refer to both the nodes except the root and the lines. We will define the following nodal and branch quantities :

For each node $i \in \mathcal{N}$, we define :

- v_i as the square of the norm of the complex voltage at that node,
- $s_i = p_i + \mathbf{i}q_i$ as the complex net power injection (the net injection being the power consumed minus the power produced)
- d_i is the active net power injection demanded at node i , i.e. the power that the agent at that node wants to reinject in the network. It is thus different than the power that will actually be seen by the network (that is, p_i) as some curtailment mechanisms can take place. This will be further discussed later. d_i is positive when the power is injected and negative if it is retrieved.

For each line $i \in \mathcal{N}_+$, we define :

- $z_i = r_i + \mathbf{i}x_i$ as the complex impedance,
- l_i as the square of the norm of the complex current,
- $S_i = P_i + \mathbf{i}Q_i$ as the sending-end complex power, where P_i denotes the active power and Q_i the reactive power.

A schematic representation of a line together with the notations we use is given below (Figure 2.1).

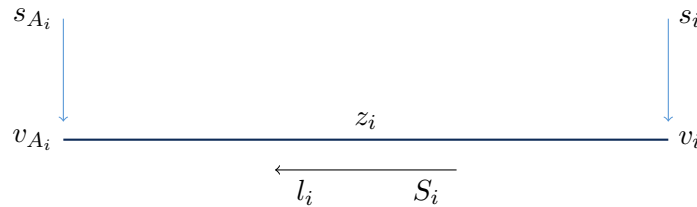


Figure 2.1: Schematic representation of a line.

We consider the OPF problem in a multi-time-step framework. This means that the variables are defined at each time step and that the constraints need to be satisfied at each of these time steps, too. We consider a horizon of T time steps. The set of time steps is denoted by \mathcal{T} and each one is represented by a positive integer, i.e. $\mathcal{T} = \{1, \dots, T\}$.

The OPF problem is in general a hard nonlinear problem for which many relaxations and algorithms have been developed since it was first formulated more than 50 years ago. A popular relaxation that linearizes the OPF is called DCOPF, where DC stands for direct current. It assumes that all voltage magnitudes are fixed and all voltage angles are close to zero. This relaxation is suitable to approximate high-voltage transmission systems for which these assumptions are realistic. However, it fails to approximate distribution systems, which are the object of our work. Instead, Masoud Farivar and Steven H. Low proposed in [6] and [7] two formulations of the general ACOPF that received a lot of attention in the community. These formulations are exact under some assumptions. I will present them in the two following subsections.

2.1.1 Angle relaxation

The first formulation they proposed is a relaxation of the voltage and current angles that yields a nonconvex quadratic program. The relaxation is exact under the following assumption :

(A₁) The graph underlying the network is a tree (also called radial network in power system engineering). As stated above, this is often the case in distribution systems and is an assumption of our work.

As mentioned earlier, the objective function of the OPF problem is often to minimize the losses or the costs. In this work, we will consider the minimization of the power losses due to the resistance of the lines. These losses will be weighted by a cost denoted by C_l so that the objective function is expressed in Euros. This will be helpful later when we will add other terms to the objective.

Farivar and Low's formulation, over the variables $\{P, Q, p, q, l, v\}$ can be written as

Model 1 Alternating Current Optimal Power Flow (AC-OPF)

Minimize:

$$C_l \sum_{j \in \mathcal{N}_+, t \in \mathcal{T}} (r_j l_{j,t}) \quad (2.1a)$$

Subject to:

$$0 = p_{0,t} + \sum_{j \in \mathcal{C}_0} (P_{j,t} - r_j l_{j,t}), \quad \forall t \in \mathcal{T} \quad (2.1b)$$

$$0 = q_{0,t} + \sum_{j \in \mathcal{C}_0} (Q_{j,t} - x_j l_{j,t}), \quad \forall t \in \mathcal{T} \quad (2.1c)$$

$$v_{\mathcal{A}_i,t} = v_{i,t} - 2(r_i P_{i,t} + x_i Q_{i,t}) + (r_i^2 + x_i^2) l_{i,t}, \quad \forall i \in \mathcal{N}_+, \forall t \in \mathcal{T} \quad (2.1d)$$

$$P_{i,t} = p_{i,t} + \sum_{j \in \mathcal{C}_i} (P_{j,t} - r_j l_{j,t}), \quad \forall i \in \mathcal{N}_+, \forall t \in \mathcal{T} \quad (2.1e)$$

$$Q_{i,t} = q_{i,t} + \sum_{j \in \mathcal{C}_i} (Q_{j,t} - x_j l_{j,t}), \quad \forall i \in \mathcal{N}_+, \forall t \in \mathcal{T} \quad (2.1f)$$

$$v_{i,t} l_{i,t} = P_{i,t}^2 + Q_{i,t}^2, \quad \forall i \in \mathcal{N}_+, \forall t \in \mathcal{T} \quad (2.1g)$$

$$\underline{v} \leq v_{i,t} \leq \bar{v}, \quad \forall i \in \mathcal{N}, \forall t \in \mathcal{T} \quad (2.1h)$$

$$0 \leq l_{i,t} \leq \bar{l}, \quad \forall i \in \mathcal{N}_+, \forall t \in \mathcal{T} \quad (2.1i)$$

$$\underline{p} \leq p_{i,t} \leq \bar{p}, \quad \forall i \in \mathcal{N}, \forall t \in \mathcal{T} \quad (2.1j)$$

Constraint (2.1j) represents flexibility in the net injection that is available due to for instance solar production or flexible load. Note that $p_{0,t}$ is the power injected in the distribution network from the transmission network. In this work, we focus on the DSO and we will thus omit questions related to the coordination between the DSO and the TSO. We consider that $p_{0,t}$ can be obtained without restrictions and for free.

Moreover, we will also focus on questions related to active power control. Therefore, we will assume that reactive power is controlled independently, by allowing some reactive power generation/-consumption at each node for free.

We will denote by $\text{AC-OPF}(p_{i,t})$ the set of constraints (2.1b) to (2.1i).

2.1.2 SOCP relaxation

The idea is now to further relax the problem to obtain an SOCP formulation for which an optimal solution can be found much more efficiently. The relaxation is performed as follows : constraint (2.1g) is replaced by

$$v_{i,t}l_{i,t} \geq P_{i,t}^2 + Q_{i,t}^2, \quad \forall i \in \mathcal{N}_+, \forall t \in \mathcal{T}$$

which is a convex constraint and can in turn be rewritten into the following SOCP constraint :

$$\begin{pmatrix} v_{i,t} + l_{i,t} \\ v_{i,t} - l_{i,t} \\ 2P_{i,t} \\ 2Q_{i,t} \end{pmatrix} \in \mathbb{L}^3, \quad \forall i \in \mathcal{N}_+, \forall t \in \mathcal{T}$$

where \mathbb{L}^3 is a third order Lorentz cone. This relaxation is exact under the following assumption :

(A₂) There is no lower bound on the active power consumption at each node, i.e. the load can always be oversatisfied.

The OPF problem becomes :

$$\begin{aligned} \min C_l \sum_{j \in \mathcal{N}_+, t \in \mathcal{T}} (r_j l_{j,t}) \\ \text{s.t. (2.1b) to (2.1f), (2.1h), (2.1i)} \\ \begin{pmatrix} v_{i,t} + l_{i,t} \\ v_{i,t} - l_{i,t} \\ 2P_{i,t} \\ 2Q_{i,t} \end{pmatrix} \in \mathbb{L}^3, \quad \forall i \in \mathcal{N}_+, \forall t \in \mathcal{T} & \quad (2.2a) \\ p_{i,t} \leq d_{i,t}, \quad \forall i \in \mathcal{N}_+, \forall t \in \mathcal{T} & \quad (2.2b) \end{aligned}$$

Recall that $d_{i,t}$ is the active power that people at node i want to inject in the network. It is considered as an input parameter of the problem. Notice also that assumption (A₂) is respected as there is no lower bound on $p_{i,t}$. The relaxation is thus exact. Constraint (2.2b) means that the demand at node i and time t should be met when possible, but we also allow unbounded consumption of power at each node so that the relaxation is exact. We will denote by $\text{SOCP-OPF}(p_{i,t})$ the set of constraints (2.1b) to (2.1f), (2.1h), (2.1i) and (2.2a).

2.2 Fuse limits

For the time being, network constraints are controlled by resorting extensively to solar and wind production curtailment. This ensures the quality of the electricity provided at the cost of throwing away free green energy. This is a huge shortfall for the DSO and more globally for the society in general for the purpose of achieving its goals in terms of cheap green energy production. For example, California had to curtail 3% of its total potential wind and power generation in the first quarter of 2017 [8]. During some peak production hours, curtailment can exceed 30% of the total solar

generation. Moreover, this curtailment is on the rise. Still in California, from 187,000 MWh in 2015, the wind and solar power curtailment reached 308,000 MWh in 2016. Not to mention also that, as discussed in section 1.2, it is the role of the DSO to provide guarantees on its services and to ensure that residential producers will be able to reinject their additional power produced in the grid.

In this context, we state that the DSO can increase the reliability of the services it provides by restricting the scope of these services. More specifically, we will in this section investigate the use of limits on consumption and reinjection of power from and in the network (hereafter referred to as fuse limits) by describing how they can be added to our model.

We model fuse limits by two variables \overline{K} and \underline{K} , corresponding respectively to an upper and a lower bound on the net injection at each node. These variables are independent of the nodes of the network and the time steps and are thus decided once and for all. Once these limits are announced, the prosumers should respect them. In case of overproduction, it will be curtailed automatically by the DSO. In case of overconsumption, the demand will not be satisfied. In what follows, they will be both referred to by the general term of curtailment.

We will use the following notation :

- $x_{i,t}^+$ is the curtailment performed at node i and time t due to overproduction,
- $x_{i,t}^-$ is the curtailment performed at node i and time t due to overconsumption,

To satisfy the fuse limits, the following constraints will have to be added to the model :

$$p_{i,t} \leq \overline{K}, \quad \forall i \in \mathcal{N}_+, \quad \forall t \in \mathcal{T} \quad (2.3a)$$

$$p_{i,t} \geq \underline{K}, \quad \forall i \in \mathcal{N}_+, \quad \forall t \in \mathcal{T} \quad (2.3b)$$

$$d_{i,t} - x_{i,t}^+ + x_{i,t}^- = p_{i,t}, \quad \forall i \in \mathcal{N}_+, \quad \forall t \in \mathcal{T} \quad (2.3c)$$

These constraints are added to model 1. Note that the curtailment variables can be used in two very different cases. The first one is to curtail $d_{i,t}$ when it is outside the fuse limits, in order to respect constraints (2.3a) and (2.3b). We will call this curtailment the *planned curtailment*, because the fuse limits are announced in advance and the customers can thus know that if they go beyond these limits, they will be curtailed. The second one can happen even when $d_{i,t}$ is inside the fuse limits and is used to respect voltage and current constraints. The latter is similar to curtailment that is used by network operators for the moment. It will be called *unplanned curtailment*.

Let us first be more specific about the definitions of planned and unplanned curtailment :

$$\text{planned curtailment} := x_{\text{planned}} = \sum_{i,t | d_{i,t} \geq \overline{K}} (d_{i,t} - \overline{K}) + \sum_{i,t | d_{i,t} \leq \underline{K}} (\underline{K} - d_{i,t})$$

$$\text{unplanned curtailment} := x_{\text{unplanned}} = \sum_{i,t} (x_{i,t}^+ + x_{i,t}^-) - x_{\text{planned}}$$

We still have to come up with a strategy to decide on suitable values for the fuse limits \overline{K} and \underline{K} . What we want is that the fuse limits increase significantly the reliability of the service provided by the DSO, i.e. that it decreases curtailment. However, it is unrealistic to choose them such that it completely removes the curtailment as it would lead to very small fuse limits, reducing considerably the scope of services provided by the DSO. Instead, we will impose that the unplanned curtailment remains at a reasonable fraction of the unplanned curtailment that would take place if there were no fuse limits. We set this fraction to 10%. With still the objective to minimize the losses, the problem that we are facing could be written as :

$$\min C_l \sum_{j \in \mathcal{N}_+, t \in \mathcal{T}} (r_j l_{j,t}) \quad (2.4a)$$

$$\text{s.t. } p_{i,t} \leq \bar{K}, \quad \forall i \in \mathcal{N}_+, \forall t \in \mathcal{T} \quad (2.4b)$$

$$p_{i,t} \geq \underline{K}, \quad \forall i \in \mathcal{N}_+, \forall t \in \mathcal{T} \quad (2.4c)$$

$$d_{i,t} - x_{i,t}^+ + x_{i,t}^- = p_{i,t}, \quad \forall i \in \mathcal{N}_+, \forall t \in \mathcal{T} \quad (2.4d)$$

$$\text{AC-OPF}(p_{i,t}) \quad (2.4e)$$

$$\bar{K}, \underline{K} \text{ s.t. unplanned curtailment} = 0.1 \text{ unplanned curtailment without fuse limits} \quad (2.4f)$$

Constraint (2.4f) cannot be easily formulated without resorting to additional integer variables, as variables $x_{i,t}^+$ and $x_{i,t}^-$ in the current model are the total curtailment and not the unplanned curtailment. Instead of resorting to integer variables, we developed a strategy to find a solution respecting constraint (2.4f) that we describe in what follows.

Let $x_{\text{unplanned, nofuse}}$ be the total unplanned curtailment obtained when there are no fuse limits, i.e. when the cost of fuse is set to 0. We also define the percentage of unplanned curtailment as :

$$\text{percentage of unplanned curtailment} := x_{\text{unplanned}}^{\%} = \frac{x_{\text{unplanned}}}{x_{\text{unplanned, nofuse}}}$$

Variables \bar{K} and \underline{K} are added in the objective with a cost, denoted by C_f . The total curtailment is also added in the objective with a cost. The cost of curtailment due to overconsumption is set to the Value Of Lost Load (VOLL).

Definition 1. *The VOLL is the value that on average, consumers would be willing to pay to avoid an outage. It is a measure of the average value of power to consumers.*

The cost of curtailment due to overproduction is called C_+ and will be in general lower than VOLL. It remains to find the value of C_f that will lead to a proportion of unplanned curtailment of 10% of the unplanned curtailment without fuse limits. The model becomes :

Model 2 Fuse Limited Optimal Power Flow (FL-OPF)

Minimize:

$$C_f(\bar{K} - \underline{K}) + C_+ \left(\sum_{i \in \mathcal{N}_+, t \in \mathcal{T}} x_{i,t}^+ \right) + \text{VOLL} \left(\sum_{i \in \mathcal{N}_+, t \in \mathcal{T}} x_{i,t}^- \right) + C_l \sum_{j \in \mathcal{N}_+, t \in \mathcal{T}} (r_j l_{j,t}) \quad (2.5a)$$

Subject to:

$$p_{i,t} \leq \bar{K}, \quad \forall i \in \mathcal{N}_+, \forall t \in \mathcal{T} \quad (2.5b)$$

$$p_{i,t} \geq \underline{K}, \quad \forall i \in \mathcal{N}_+, \forall t \in \mathcal{T} \quad (2.5c)$$

$$d_{i,t} - x_{i,t}^+ + x_{i,t}^- = p_{i,t}, \quad \forall i \in \mathcal{N}_+, \forall t \in \mathcal{T} \quad (2.5d)$$

$$\text{AC-OPF}(p_{i,t}) \quad (2.5e)$$

To understand this model, observe that when C_f is set to 0, the optimal solution is to set \bar{K} to a value greater than the maximum demanded injection $d_{i,t}$ and \underline{K} lower than the minimum of $d_{i,t}$, so

that no planned curtailment will have to take place and all the curtailment is unplanned curtailment. In this case, $x_{\text{unplanned}}^{\%}$ is equal to 1. As C_f becomes larger, there is always a value above which the optimal values of \bar{K} and \underline{K} are both 0 and all the curtailment is planned curtailment, which implies that there are no unplanned curtailment. In this case, $x_{\text{unplanned}}^{\%}$ is equal to 0. We can hope to find an intermediate value of C_f that will lead to a fixed value of $x_{\text{unplanned}}^{\%}$, here 0.1. The way to find the right value of C_f in order to match the constraint (2.4f) will be explained in chapter 3 dedicated to the solution strategy.

2.3 Line reinforcement

Another decision that the DSO can make to improve the operations of its network is to reinforce it, i.e. to build new lines with larger capacity and smaller impedance. Allowing the DSO to decide on the impedance of the lines complicates the model. Indeed, if r_j, x_j and \bar{l}_j become variables, the AC-OPF constraints that were linear in model (1) would become nonlinear, which would greatly reduce the chances of finding a solution in reasonable time. Therefore, we will not consider the possibility for continuous line reinforcement but instead consider that there is a finite set of line choices that the DSO can make, each choice being associated to a known impedance, current limit and cost.

Let

- N_{choices} be the number of different choices that we have for the lines,
- \mathcal{G} be the set of choices $\{1, \dots, N_{\text{choices}}\}$,
- I_g, r_g, x_g, C_g be respectively the maximum current allowed, the resistance, the reactance and the cost per unit of length for each choice $g \in \mathcal{G}$,
- w_g be a binary variable equal to 1 if choice g is made, 0 otherwise for each possible choice $g \in \mathcal{G}$,
- \bar{l}_j the length of line j .

Note that in this work, we suppose that there is an existing distribution network and we don't consider the case where the network has to be built from scratch. I_1, r_1 and x_1 are thus the characteristics of the existing lines and C_1 is set to 0. Note also that we consider a unique type of line for the whole network.

Then, the problem of line reinforcement subject to AC-OPF constraints can be written as follows :

$$\min \sum_{j \in \mathcal{N}_+, g \in \mathcal{G}} w_g \bar{L}_j C_g \quad (2.6a)$$

$$\text{s.t. } 0 = p_{0,t} + \sum_{j \in \mathcal{C}_0} \left(P_{j,t} - \left(\sum_{g \in \mathcal{G}} w_g \bar{L}_j r_g \right) l_{j,t} \right), \quad \forall t \in \mathcal{T} \quad (2.6b)$$

$$0 = q_{0,t} + \sum_{j \in \mathcal{C}_0} \left(Q_{j,t} - \left(\sum_{g \in \mathcal{G}} w_g \bar{L}_j x_g \right) l_{j,t} \right), \quad \forall t \in \mathcal{T} \quad (2.6c)$$

$$v_{\mathcal{A}_i,t} = v_{i,t} - 2 \left(\left(\sum_{g \in \mathcal{G}} w_g \bar{L}_i r_g \right) P_{i,t} + \left(\sum_{g \in \mathcal{G}} w_g \bar{L}_i x_g \right) Q_{i,t} + \left(\sum_{g \in \mathcal{G}} w_g \bar{L}_i^2 (r_g^2 + x_g^2) \right) l_{i,t} \right), \quad (2.6d)$$

$$\forall i \in \mathcal{N}_+, \forall t \in \mathcal{T}$$

$$P_{i,t} = p_{i,t} + \sum_{j \in \mathcal{C}_i} \left(P_{j,t} - \left(\sum_{g \in \mathcal{G}} w_g \bar{L}_j r_g \right) l_{j,t} \right), \quad \forall i \in \mathcal{N}_+, \forall t \in \mathcal{T} \quad (2.6e)$$

$$Q_{i,t} = q_{i,t} + \sum_{j \in \mathcal{C}_i} \left(Q_{j,t} - \left(\sum_{g \in \mathcal{G}} w_g \bar{L}_j x_g \right) l_{j,t} \right), \quad \forall i \in \mathcal{N}_+, \forall t \in \mathcal{T} \quad (2.6f)$$

$$v_{i,t} l_{i,t} = P_{i,t}^2 + Q_{i,t}^2, \quad \forall i \in \mathcal{N}_+, \forall t \in \mathcal{T} \quad (2.6g)$$

$$\underline{v} \leq v_{i,t} \leq \bar{v}, \quad \forall i \in \mathcal{N}, \forall t \in \mathcal{T} \quad (2.6h)$$

$$0 \leq l_{i,t} \leq \sum_{g \in \mathcal{G}} w_g I_g, \quad \forall i \in \mathcal{N}_+, \forall t \in \mathcal{T} \quad (2.6i)$$

$$\sum_{g \in \mathcal{G}} w_g = 1 \quad (2.6j)$$

$$w_g \text{ binary}, \quad \forall g \in \mathcal{G} \quad (2.6k)$$

Note that even for the continuous relaxation, equations (2.6b) to (2.6f) are still nonlinear as w_g is a variable. By extending the formulation with new variables, we can restore their linearity as follows :

Let

- \bar{P} and \underline{P} be an upper and lower bound on the active branch power,
- \bar{Q} and \underline{Q} be an upper and lower bound on the reactive branch power,
- $\tilde{P}_{i,t,g}, \tilde{Q}_{i,t,g}, \tilde{l}_{i,t,g}$ be new branch power and current variables equal to respectively $P_{i,t}, Q_{i,t}, l_{i,t}$ if choice g is made and 0 otherwise, for each choice $g \in \mathcal{G}$.

Note that $I_{N_{\text{choices}}}$ and 0 are respectively upper and lower bounds on the branch currents. We write the problem as follows :

Model 3 Distribution Network Reinforcement (DNR)

Minimize:

$$\sum_{j \in \mathcal{N}_+, g \in \mathcal{G}} w_g \bar{L}_j C_g \quad (2.7a)$$

Subject to:

$$0 = p_{0,t} + \sum_{j \in \mathcal{C}_0} \left(P_{j,t} - \left(\sum_{g \in \mathcal{G}} \bar{L}_j r_g \tilde{l}_{j,t,g} \right) \right), \quad \forall t \in \mathcal{T} \quad (2.7b)$$

$$0 = q_{0,t} + \sum_{j \in \mathcal{C}_0} \left(Q_{j,t} - \left(\sum_{g \in \mathcal{G}} \bar{L}_j x_g \tilde{l}_{j,t,g} \right) \right), \quad \forall t \in \mathcal{T} \quad (2.7c)$$

$$v_{\mathcal{A},t} = v_{i,t} - 2 \left(\sum_{g \in \mathcal{G}} \bar{L}_i r_g \tilde{P}_{j,t,g} + \bar{L}_i x_g \tilde{Q}_{j,t,g} + \bar{L}_i^2 (r_g^2 + x_g^2) \tilde{l}_{i,t,g} \right), \quad \forall i \in \mathcal{N}_+, \forall t \in \mathcal{T} \quad (2.7d)$$

$$P_{i,t} = p_{i,t} + \sum_{j \in \mathcal{C}_i} \left(P_{j,t} - \left(\sum_{g \in \mathcal{G}} \bar{L}_j r_g \tilde{l}_{j,t,g} \right) \right), \quad \forall i \in \mathcal{N}_+, \forall t \in \mathcal{T} \quad (2.7e)$$

$$Q_{i,t} = q_{i,t} + \sum_{j \in \mathcal{C}_i} \left(Q_{j,t} - \left(\sum_{g \in \mathcal{G}} \bar{L}_j x_g \tilde{l}_{j,t,g} \right) \right), \quad \forall i \in \mathcal{N}_+, \forall t \in \mathcal{T} \quad (2.7f)$$

$$v_{i,t} l_{i,t} = P_{i,t}^2 + Q_{i,t}^2, \quad \forall i \in \mathcal{N}_+, \forall t \in \mathcal{T} \quad (2.7g)$$

$$\underline{v} \leq v_{i,t} \leq \bar{v}, \quad \forall i \in \mathcal{N}, \forall t \in \mathcal{T} \quad (2.7h)$$

$$0 \leq l_{i,t} \leq \sum_{g \in \mathcal{G}} w_g I_g, \quad \forall i \in \mathcal{N}_+, \forall t \in \mathcal{T} \quad (2.7i)$$

$$\sum_{g \in \mathcal{G}} w_g = 1 \quad (2.7j)$$

$$w_g \text{ binary}, \quad \forall g \in \mathcal{G} \quad (2.7k)$$

$$\underline{P} w_g \leq \tilde{P}_{j,t,g} \leq \bar{P} w_g, \quad \forall j \in \mathcal{N}_+, \forall t \in \mathcal{T}, \forall g \in \mathcal{G} \quad (2.7l)$$

$$P_{j,t} - (1 - w_g) \bar{P} \leq \tilde{P}_{j,t,g} \leq P_{j,t} - (1 - w_g) \underline{P}, \quad \forall j \in \mathcal{N}_+, \forall t \in \mathcal{T}, \forall g \in \mathcal{G} \quad (2.7m)$$

$$\underline{Q} w_g \leq \tilde{Q}_{j,t,g} \leq \bar{Q} w_g, \quad \forall j \in \mathcal{N}_+, \forall t \in \mathcal{T}, \forall g \in \mathcal{G} \quad (2.7n)$$

$$Q_{j,t} - (1 - w_g) \bar{Q} \leq \tilde{Q}_{j,t,g} \leq Q_{j,t} - (1 - w_g) \underline{Q}, \quad \forall j \in \mathcal{N}_+, \forall t \in \mathcal{T}, \forall g \in \mathcal{G} \quad (2.7o)$$

$$0 \leq \tilde{l}_{j,t,g} \leq I_{N_{\text{choices}}} w_g, \quad \forall j \in \mathcal{N}_+, \forall t \in \mathcal{T}, \forall g \in \mathcal{G} \quad (2.7p)$$

$$l_{j,t} - (1 - w_g) I_{N_{\text{choices}}} \leq \tilde{l}_{j,t,g} \leq l_{j,t}, \quad \forall j \in \mathcal{N}_+, \forall t \in \mathcal{T}, \forall g \in \mathcal{G} \quad (2.7q)$$

This model can be understood with the following observations : when w_g is equal to 0, equation (2.7l) imposes that $\tilde{P}_{j,t,g} = 0$ while equation (2.7m) becomes

$$P_{j,t} - \bar{P} \leq \tilde{P}_{j,t,g} \leq P_{j,t} - \underline{P}$$

which is trivially satisfied in view of the definition of \bar{P} and \underline{P} and the fact that $\tilde{P}_{j,t,g} = 0$. When w_g is equal to 1, equation (2.7l) becomes

$$\underline{P} \leq \tilde{P}_{j,t,g} \leq \bar{P}$$

which is trivially satisfied in view of the definition of $\tilde{P}_{j,t,g}$, \bar{P} and \underline{P} . Equation (2.7m) forces $\tilde{P}_{j,t,g}$ to be equal to $P_{j,t}$. The same logic applies to $\tilde{Q}_{j,t,g}$ and $\tilde{l}_{j,t,g}$.

Observe that now, the only sources of nonconvexity are the binary restriction on w_g and equation (2.7g).

2.4 Storage capacity investment

The third possibility that the DSO has is to invest in storage capacity. This can be modeled as follows, let

- $e_{i,t}, \forall i \in \mathcal{N}, t \in \mathcal{T}$ be the energy stored at node i and time t ,
- $f_i, \forall i \in \mathcal{N}$ be the storage investment/maximal storage capacity at node i ,
- $p_{i,t}^{in}, \forall i \in \mathcal{N}, t \in \mathcal{T}$ be the active power input to be stored at node i and time t ,
- $p_{i,t}^{out}, \forall i \in \mathcal{N}, t \in \mathcal{T}$ be the active power output from the battery at node i and time t ,
- \underline{p}_i^{in} and \overline{p}_i^{in} be respectively a lower bound and an upper bound on the active power input at node i ,
- \underline{p}_i^{out} and \overline{p}_i^{out} be respectively a lower bound and an upper bound on the active power input at node i ,
- h is the duration of a time step,
- ξ_{in} and ξ_{out} are respectively a charging and a discharging factor,
- C_s be the cost of having 1 unit of storage available by unit of time,
- \mathcal{T}_+ be the set of time steps except the first one,
- \mathcal{T}_- be the set of time steps except the last one.

Then, the problem reads as follows:

Model 4 Storage Investment (SI)

Minimize:

$$C_l \sum_{j \in \mathcal{N}_+, t \in \mathcal{T}} (r_j l_{j,t}) + C_s \sum_{i \in \mathcal{N}, t \in \mathcal{T}} f_i \quad (2.8a)$$

Subject to:

$$0 = p_{0,t} + \sum_{j \in \mathcal{C}_0} (P_{j,t} - r_j l_{j,t}), \quad \forall t \in \mathcal{T} \quad (2.8b)$$

$$0 = q_{0,t} + \sum_{j \in \mathcal{C}_0} (Q_{j,t} - x_j l_{j,t}), \quad \forall t \in \mathcal{T} \quad (2.8c)$$

$$v_{\mathcal{A}_i,t} = v_{i,t} - 2(r_i P_{i,t} + x_i Q_{i,t}) + (r_i^2 + x_i^2) l_{i,t}, \quad \forall i \in \mathcal{N}_+, \forall t \in \mathcal{T} \quad (2.8d)$$

$$P_{i,t} + p_{i,t}^{in} - p_{i,t}^{out} = p_{i,t} + \sum_{j \in \mathcal{C}_i} (P_{j,t} - r_j l_{j,t}), \quad \forall i \in \mathcal{N}_+, \forall t \in \mathcal{T} \quad (2.8e)$$

$$Q_{i,t} = q_{i,t} + \sum_{j \in \mathcal{C}_i} (Q_{j,t} - x_j l_{j,t}), \quad \forall i \in \mathcal{N}_+, \forall t \in \mathcal{T} \quad (2.8f)$$

$$v_{i,t} l_{i,t} = P_{i,t}^2 + Q_{i,t}^2, \quad \forall i \in \mathcal{N}_+, \forall t \in \mathcal{T} \quad (2.8g)$$

$$\underline{v} \leq v_{i,t} \leq \bar{v}, \quad \forall i \in \mathcal{N}, \forall t \in \mathcal{T} \quad (2.8h)$$

$$0 \leq l_{i,t} \leq \bar{l}, \quad \forall i \in \mathcal{N}_+, \forall t \in \mathcal{T} \quad (2.8i)$$

$$0 \leq e_{i,t} \leq f_i, \quad \forall i \in \mathcal{N}, \forall t \in \mathcal{T} \quad (2.8j)$$

$$\underline{p}_i^{in} \leq p_{i,t}^{in} \leq \bar{p}_i^{in}, \quad \forall i \in \mathcal{N}, \forall t \in \mathcal{T} \quad (2.8k)$$

$$\underline{p}_i^{out} \leq p_{i,t}^{out} \leq \bar{p}_i^{out}, \quad \forall i \in \mathcal{N}, \forall t \in \mathcal{T} \quad (2.8l)$$

$$e_{i,t} = e_{i,t-1} + h \left(\xi_{in} p_{i,t}^{in} - \frac{1}{\xi_{out}} p_{i,t}^{out} \right), \quad \forall i \in \mathcal{N}, \forall t \in \mathcal{T}_+ \quad (2.8m)$$

$$e_{i,1} = 0, \quad \forall i \in \mathcal{N} \quad (2.8n)$$

2.5 Optimal DSO planning

By combining the AC-OPF constraints and the modeling of the decision on fuse limits, line reinforcement and storage investment, we can formulate the problem of optimal planning of the DSO grid, called Optimal DSO Planning (ODP), in the following way :

Model 5 Optimal DSO Planning (ODP)

Minimize:

$$C_f(\bar{K} - \underline{K}) + C_+(\sum_{i,t} x_{i,t}^+) + VOLL(\sum_{i,t} x_{i,t}^-) + \sum_{g,j} (w_g \bar{L}_j C_g + \bar{L}_j r_g \tilde{l}_{j,t,g}) + C_s \sum_{i,t} f_i \quad (2.9a)$$

Subject to:

$$\sum_{g \in \mathcal{G}} w_g = 1 \quad (2.9b)$$

$$w_g \text{ binary}, \quad \forall g \in \mathcal{G} \quad (2.9c)$$

$$p_{0,t}^{in} - p_{0,t}^{out} = p_{0,t} + \sum_{j \in \mathcal{C}_0} \left(P_{j,t} - \left(\sum_{g \in \mathcal{G}} \bar{L}_j r_g \tilde{l}_{j,t,g} \right) \right), \quad \forall t \in \mathcal{T} \quad (2.9d)$$

$$0 = q_{0,t} + \sum_{j \in \mathcal{C}_0} \left(Q_{j,t} - \left(\sum_{g \in \mathcal{G}} \bar{L}_j x_g \tilde{l}_{j,t,g} \right) \right), \quad \forall t \in \mathcal{T} \quad (2.9e)$$

$$v_{\mathcal{A},t} = v_{i,t} - 2 \left(\sum_{g \in \mathcal{G}} \bar{L}_i r_g \tilde{P}_{i,t,g} + \bar{L}_i x_g \tilde{Q}_{i,t,g} + \bar{L}_i^2 (r_g^2 + x_g^2) \tilde{l}_{i,t,g} \right), \quad \forall i \in \mathcal{N}_+, \quad \forall t \in \mathcal{T} \quad (2.9f)$$

$$P_{i,t} + p_{i,t}^{in} - p_{i,t}^{out} = p_{i,t} + \sum_{j \in \mathcal{C}_i} \left(P_{j,t} - \left(\sum_{g \in \mathcal{G}} \bar{L}_j r_g \tilde{l}_{j,t,g} \right) \right), \quad \forall i \in \mathcal{N}_+, \quad \forall t \in \mathcal{T} \quad (2.9g)$$

$$Q_{i,t} = q_{i,t} + \sum_{j \in \mathcal{C}_i} \left(Q_{j,t} - \left(\sum_{g \in \mathcal{G}} \bar{L}_j x_g \tilde{l}_{j,t,g} \right) \right), \quad \forall i \in \mathcal{N}_+, \quad \forall t \in \mathcal{T} \quad (2.9h)$$

$$v_{i,t} l_{i,t} = P_{i,t}^2 + Q_{i,t}^2, \quad \forall i \in \mathcal{N}_+, \quad \forall t \in \mathcal{T} \quad (2.9i)$$

$$\underline{v} \leq v_{i,t} \leq \bar{v}, \quad \forall i \in \mathcal{N}, \quad \forall t \in \mathcal{T} \quad (2.9j)$$

$$\underline{K} \leq p_{i,t} \leq \bar{K}, \quad \forall i \in \mathcal{N}_+, \quad \forall t \in \mathcal{T} \quad (2.9k)$$

$$d_{i,t} - x_{i,t}^+ + x_{i,t}^- = p_{i,t}, \quad \forall i \in \mathcal{N}_+, \quad \forall t \in \mathcal{T} \quad (2.9l)$$

$$x_{i,t}^+ \geq 0, \quad \forall i \in \mathcal{N}_+, \quad \forall t \in \mathcal{T} \quad (2.9m)$$

$$x_{i,t}^- \geq 0, \quad \forall i \in \mathcal{N}_+, \quad \forall t \in \mathcal{T} \quad (2.9n)$$

$$0 \leq l_{i,t} \leq \sum_{g \in \mathcal{G}} w_g I_g, \quad \forall i \in \mathcal{N}_+, \quad \forall t \in \mathcal{T} \quad (2.9o)$$

$$\underline{P} w_g \leq \tilde{P}_{j,t,g} \leq \bar{P} w_g, \quad \forall j \in \mathcal{N}_+, \quad \forall t \in \mathcal{T}, \quad \forall g \in \mathcal{G} \quad (2.9p)$$

$$P_{j,t} - (1 - w_g) \bar{P} \leq \tilde{P}_{j,t,g} \leq P_{j,t} - (1 - w_g) \underline{P}, \quad \forall j \in \mathcal{N}_+, \quad \forall t \in \mathcal{T}, \quad \forall g \in \mathcal{G} \quad (2.9q)$$

$$\underline{Q} w_g \leq \tilde{Q}_{j,t,g} \leq \bar{Q} w_g, \quad \forall j \in \mathcal{N}_+, \quad \forall t \in \mathcal{T}, \quad \forall g \in \mathcal{G} \quad (2.9r)$$

$$0 \leq \tilde{l}_{j,t,g} \leq I_{N_{\text{choices}}} w_g, \quad \forall j \in \mathcal{N}_+, \quad \forall t \in \mathcal{T}, \quad \forall g \in \mathcal{G} \quad (2.9s)$$

$$Q_{j,t} - (1 - w_g) \bar{Q} \leq \tilde{Q}_{j,t,g} \leq Q_{j,t} - (1 - w_g) \underline{Q}, \quad \forall j \in \mathcal{N}_+, \quad \forall t \in \mathcal{T}, \quad \forall g \in \mathcal{G} \quad (2.9t)$$

$$l_{j,t} - (1 - w_g) I_{N_{\text{choices}}} \leq \tilde{l}_{j,t,g} \leq l_{j,t}, \quad \forall j \in \mathcal{N}_+, \quad \forall t \in \mathcal{T}, \quad \forall g \in \mathcal{G} \quad (2.9u)$$

$$0 \leq e_{i,t} \leq f_i, \quad \forall i \in \mathcal{N}, \quad \forall t \in \mathcal{T} \quad (2.9v)$$

$$\underline{p}_i^{in} \leq p_{i,t}^{in} \leq \bar{p}_i^{in}, \quad \forall i \in \mathcal{N}, \quad \forall t \in \mathcal{T} \quad (2.9w)$$

$$\underline{p}_i^{out} \leq p_{i,t}^{out} \leq \bar{p}_i^{out}, \quad \forall i \in \mathcal{N}, \quad \forall t \in \mathcal{T} \quad (2.9x)$$

$$e_{i,t} = e_{i,t-1} + h \left(\xi_{in} p_{i,t-1}^{in} - \frac{1}{\xi_{out}} p_{i,t-1}^{out} \right), \quad \forall i \in \mathcal{N}, \quad \forall t \in \mathcal{T}_+ \quad (2.9y)$$

$$e_{i,1} = 0, \quad \forall i \in \mathcal{N} \quad (2.9z)$$

2.6 Robust formulation

Our goal is to find a solution to this problem that will be robust to load and generation uncertainties. Let us first reformulate the problem as a robust optimization problem. The uncertainty is in the demand parameter $d_{i,t}$. Let us denote by \mathcal{D} the uncertainty set of the demand so that $d_{i,t} \in \mathcal{D} \forall i \in \mathcal{N}_+, \forall t \in \mathcal{T}$. As this demand is uncertain, it is now considered as a variable.

We now separate the variables into first-stage and second-stage variables. First-stage variables, denoted by \mathbf{x} are decisions that have to be made before knowledge of the realization of the uncertainty. Second-stage variables, denoted by \mathbf{y} , are the remaining variables and correspond to the decisions that are made after realization of the uncertainty. We do the separation as follows :

- $\mathbf{x} = \{\underline{K}, \overline{K}, w_g, f_i \forall g \in \mathcal{G}, \forall i \in \mathcal{N}\}$
- $\mathbf{y} = \{x_{i,t}^+, x_{i,t}^-, p_{i,t}, P_{j,t}, Q_{j,t}, v_{i,t}, l_{j,t}, \tilde{P}_{j,t,g}, \tilde{Q}_{j,t,g}, \tilde{l}_{j,t,g}, e_{i,t}, p_{i,t}^{in}, p_{i,t}^{out}, \forall g \in \mathcal{G}, \forall i \in \mathcal{N}, \forall j \in \mathcal{N}_+, \forall t \in \mathcal{T}\}$

We also denote the vector of uncertain variables by \mathbf{d} . We have $\mathbf{d} = \{d_{i,t} \forall i \in \mathcal{N}_+, \forall t \in \mathcal{T}\}$

Let us denote by \mathcal{X} the set of constraints containing only first-stage variables. We have

$$\mathcal{X} = \{\mathbf{x} : \sum_g w_g = 1, w_g \text{ binary}\}$$

Let us denote by \mathcal{Y} the set containing the remaining constraints.

$$\mathcal{Y} = \{\mathbf{x}, \mathbf{y}, \mathbf{d} \text{ subject to (2.9d) to (2.9z)}\}$$

Let $\mathcal{Y}(\mathbf{d})$ be the set \mathcal{Y} with fixed \mathbf{d} taken as a parameter and let $\mathcal{Y}(\mathbf{x}, \mathbf{d})$ be the set $\mathcal{Y}(\mathbf{d})$ with fixed \mathbf{x} taken as a parameter.

When \mathbf{d} is fixed to deterministic known values, our problem can be simply rewritten as

$$\begin{aligned} \min_{\mathbf{x}, \mathbf{y}} \mathbf{a}^\top \mathbf{x} + \mathbf{b}^\top \mathbf{y} \\ \text{s.t. } \mathbf{x} \in \mathcal{X} \\ (\mathbf{x}, \mathbf{y}) \in \mathcal{Y}(\mathbf{d}) \end{aligned} \quad (2.10)$$

with \mathbf{a} and \mathbf{b} defined correspondingly. The robust problem consists in finding the optimal value of this optimization problem subject to the worst case of the uncertainty. It can be formally written as

$$\min_{\mathbf{x} \in \mathcal{X}} \left(\mathbf{a}^\top \mathbf{x} + \max_{\mathbf{d} \in \mathcal{D}} \min_{\mathbf{y} \in \mathcal{Y}(\mathbf{x}, \mathbf{d})} \mathbf{b}^\top \mathbf{y} \right) \quad (2.11)$$

2.6.1 Uncertainty set

Let us now explain how we model the uncertainty set \mathcal{D} . We wish to be robust to the following :

- Distributed photovoltaic location and production.
- Electrical vehicles (EV) location and charging load.
- Other load.

Let's describe each subset separately.

PV location and production

Let us denote by u_i^{PV} an uncertain binary parameter indicating whether there are PV panels at node $i \in \mathcal{N}_+$. Let $d_{i,t}^{\text{PV}}$ be an uncertain parameter corresponding to the PV production at node i and time t . The traditional approach for robust optimization was developed by Soyster back in the 1970s in [9]. It consists in considering that the uncertain parameter can take any value between a lower and an upper bound. Although having the whole hypercube is optimal in terms of robustness, it is very conservative. The probability that each uncertain parameter takes its worst value is in general very low. Other models that relax slightly some robustness constraints to get a model more tractable have later been developed ([10], [3]).

In our case, the conservative approach would be to consider that each node can have PV panels installed so that the only restriction on u_i^{PV} is the binary restriction. However, the probability that each household in a distribution network have PV panels installed is low. Therefore, inspired by Bertsimas and Sim budget uncertainty set developed in [3], we propose to restrict the number of PV installations possible (Δ_1^{PV}). We thus impose the constraint

$$\sum_{i \in \mathcal{N}_+} u_i^{\text{PV}} = \Delta_1^{\text{PV}}$$

This parameter could potentially vary with time to take into account the penetration of PV systems in the grid.

Note that there is a big drawback in imposing binary restrictions in the uncertain parameter. We therefore relax this condition by allowing u_i^{PV} to be continuous in $[0, 1]$ and we suppose that it will be exact because for voltage constraints, it is worse to have all the production at the same place compared to a production that is spread in the entire network.

Now, let \bar{d}_t^{PV} be the nominal value of PV production at time t . This value is available to the DSO as a forecast value. Let also $\bar{\delta}^{\text{PV}}$ be its maximum deviation from the nominal value in percent of this nominal value. For the uncertain production $d_{i,t}^{\text{PV}}$, we also use a budget uncertainty set with the only difference that the production is imposed to be 0 when u_i^{PV} is 0. It can be expressed as

$$\left\{ d_{i,t}^{\text{PV}} \in \mathbb{R} \mid \sum_{\substack{i \in \mathcal{N}_+, u_i^{\text{PV}} \neq 0 \\ \bar{d}_t^{\text{PV}} \neq 0}} \frac{|d_{i,t}^{\text{PV}} - \bar{d}_t^{\text{PV}}|}{\bar{\delta}^{\text{PV}} \bar{d}_t^{\text{PV}}} \leq \Delta_2^{\text{PV}}, \right. \\ \left. d_{i,t}^{\text{PV}} \in \left[u_i^{\text{PV}} \left(\bar{d}_t^{\text{PV}} - \bar{\delta}^{\text{PV}} \bar{d}_t^{\text{PV}} \right), u_i^{\text{PV}} \left(\bar{d}_t^{\text{PV}} + \bar{\delta}^{\text{PV}} \bar{d}_t^{\text{PV}} \right) \right] \right\}$$

Note that we could also have used a maximum value for the deviation \hat{d}_t^{PV} that does not depend on the nominal value like the set initially proposed by Bertsimas and Sim [3]. However, in our case, it makes more sense to use a percentage of the nominal value so that when the nominal value of the solar production is zero, the worst case is also zero. Δ_2^{PV} controls the level of conservatism. It varies between 0 and Δ_1^{PV} . When it is 0, it corresponds to the deterministic case : the demand will take its nominal value in all nodes. When it is equal to Δ_1^{PV} , it is the most conservative set and corresponds to the whole hypercube for locations with PV installation.

EV location and load

The uncertainty related to Electrical Vehicle (EV) is different to the one related to PV production in that for EVs, the uncertainty is more about when in the day consumers are going to charge their

car instead of about how much power they will need to charge it. Let us in this section model the uncertainty on location and timing of charge related to EVs.

The uncertainty on location will be modeled in the same way as for PV. Let u_i^{EV} by a variable equals to 1 if node i has an EV, 0 otherwise. We will impose the number of EVs in the network :

$$\sum_{i \in \mathcal{N}_+} u_i^{\text{EV}} = \Delta^{\text{EV}}$$

For the timing of charge, we will suppose that each EV owner will have to consume everyday a fixed amount of energy, denoted by C , to charge the battery. We will denote by \mathcal{T}_d the set of time steps that belongs to a certain day d . We represent each day by a positive integer $d \in \{1, \dots, D\}$, where D is the number of days during the time period considered. Note that we have $\mathcal{T} = \cup_{d=1}^D \mathcal{T}_d$. We add the two following constraints on the EV demand :

$$\sum_{t \in \mathcal{T}_d} d_{i,t}^{\text{EV}} = u_i^{\text{EV}} C, \quad \forall i \in \mathcal{N}_+, \quad \forall d \in \{1, \dots, D\} \quad (2.12a)$$

$$d_{i,t}^{\text{EV}} \leq 1920h, \quad \forall i \in \mathcal{N}_+, \quad \forall t \in \mathcal{T} \quad (2.12b)$$

where 1920 represent the maximum power in W that one can obtain from the network and we recall that h is the duration of a time step in hours (h is equal to 1 for an hourly resolution). Constraint (2.12a) imposes that total charge is met for nodes with EV. Constraint (2.12b) ensures that the total power allowed is not exceeded.

Other load

For the usual load, there is no notion of location. We can thus model it with a simple budget constraint as

$$\left\{ \begin{array}{l} d_{i,t}^{\text{Load}} \in \mathbb{R} \mid \sum_{i \in \mathcal{N}_+} \frac{|d_{i,t}^{\text{Load}} - \bar{d}_t^{\text{Load}}|}{\hat{d}_t^{\text{Load}}} \leq \Delta^{\text{Load}}, \\ d_{i,t}^{\text{Load}} \in \left[\bar{d}_t^{\text{Load}} - \hat{d}_t^{\text{Load}}, \bar{d}_t^{\text{Load}} + \hat{d}_t^{\text{Load}} \right] \end{array} \right\}$$

In this case, Δ^{Load} takes integer values between 0 and $|\mathcal{N}_+|$.

Let us define the set of extended uncertain parameters

$$\tilde{\mathbf{d}} = \left\{ d_{i,t}, d_{i,t}^{\text{PV}}, u_i^{\text{PV}}, d_{i,t}^{\text{EV}}, u_i^{\text{EV}}, d_{i,t}^{\text{Load}} \mid i \in \mathcal{N}_+, t \in \mathcal{T} \right\}$$

Let us also denote the extended uncertainty set by $\tilde{\mathcal{D}}$. It can thus be written as

$$\begin{aligned}
\tilde{\mathcal{D}} = \left\{ \tilde{\mathbf{d}} \mid \sum_{i \in \mathcal{N}} u_i^{\text{PV}} &= \Delta_1^{\text{PV}}, \\
u_i^{\text{PV}} &\in [0, 1], \\
\sum_{\substack{i \in \mathcal{N}, u_i^{\text{PV}} \neq 0 \\ \bar{d}_t^{\text{PV}} \neq 0}} \frac{|d_{i,t}^{\text{PV}} - \bar{d}_t^{\text{PV}}|}{\bar{\delta}^{\text{PV}} \bar{d}_t^{\text{PV}}} &\leq \Delta_2^{\text{PV}}, \\
d_{i,t}^{\text{PV}} &\in \left[u_i^{\text{PV}} \left(\bar{d}_t^{\text{PV}} - \bar{\delta}^{\text{PV}} \bar{d}_t^{\text{PV}} \right), u_i^{\text{PV}} \left(\bar{d}_t^{\text{PV}} + \bar{\delta}^{\text{PV}} \bar{d}_t^{\text{PV}} \right) \right], \\
\sum_{i \in \mathcal{N}} u_i^{\text{EV}} &= \Delta^{\text{EV}}, \\
u_i^{\text{EV}} &\in [0, 1], \\
\sum_{t \in \mathcal{T}_d} d_{i,t}^{\text{EV}} &= u_i^{\text{PV}} C \\
d_{i,t}^{\text{EV}} &\leq 1920 \\
\sum_{i \in \mathcal{N}} \frac{|d_{i,t}^{\text{Load}} - \bar{d}_t^{\text{Load}}|}{\hat{d}_t^{\text{Load}}} &\leq \Delta^{\text{Load}}, \\
d_{i,t}^{\text{Load}} &\in \left[\bar{d}_t^{\text{Load}} - \hat{d}_t^{\text{Load}}, \bar{d}_t^{\text{Load}} + \hat{d}_t^{\text{Load}} \right], \\
d_{i,t} &= d_{i,t}^{\text{PV}} - d_{i,t}^{\text{EV}} - d_{i,t}^{\text{Load}} \}
\end{aligned}$$

Notice that \mathcal{D} can be defined in function of $\tilde{\mathcal{D}}$ as

$$\mathcal{D} = \left\{ \mathbf{d} \mid \exists d_{i,t}^{\text{PV}}, u_i^{\text{PV}}, d_{i,t}^{\text{EV}}, u_i^{\text{EV}}, d_{i,t}^{\text{Load}}, i \in \mathcal{N}_+, t \in \mathcal{T} \mid \tilde{\mathbf{d}} \in \tilde{\mathcal{D}} \right\}$$

Solution

This chapter is dedicated to the presentation of the solution strategy that we will use to solve the robust ODP. We first show in section 3.1 how we can solve the AC-OPF problem with a sequence of convex problems. We then explain the two-stage robust algorithm used to deal with uncertainty. After that, we present a method to find the right value of C_f to use in order to have a limited amount of unplanned curtailment, as explained in section 2.2. Finally, we conclude this chapter by deriving the dual of our problem and discussing the interpretation of some of the dual variables.

3.1 ACOPF as a sequence of SOCP

In order to develop an algorithm for solving problem (2.11), we need to express (2.10) as a conic problem. For clarity, we recall here problem (2.10) :

$$\begin{aligned} \min_{\mathbf{x}, \mathbf{y}} \quad & \mathbf{a}^\top \mathbf{x} + \mathbf{b}^\top \mathbf{y} \\ \text{s.t.} \quad & \mathbf{x} \in \mathcal{X} \\ & (\mathbf{x}, \mathbf{y}) \in \mathcal{Y}(\mathbf{d}) \end{aligned}$$

where \mathbf{d} is considered to be a deterministic known value. We will use this assumption throughout this section and it will be relaxed in the next section (section 3.2). The transformation to a conic problem will be achieved by using a technique designed by Na Li *et al.* and published in [5]. In this section I will describe this algorithm and show how it can be applied to our problem.

Their idea is to use a Convex-Concave Procedure (CCP) to restore feasibility to the solution obtained with the SOCP relaxation. There are thus two major steps : the first one uses the SOCP-OPF formulation to obtain an initial point close to the global optimal. The second step solves a sequence of problems where the nonconvex part of the quadratic constraint is linearized. A slack variable is also added to this constraint and penalized in the objective so that feasibility is recovered at the end of this step.

More formally, let us define the two following convex quadratic functions

- $f_{j,t}(\mathbf{y}) = (v_{j,t} + l_{j,t})^2$
- $g_{j,t}(\mathbf{y}) = (v_{j,t} - l_{j,t})^2 + (2P_{j,t})^2 + (2Q_{j,t})^2$

With this notation, the nonconvex quadratic constraint (2.9i), namely

$$v_{j,t} l_{j,t} = P_{j,t}^2 + Q_{j,t}^2$$

can be written as

$$f_{j,t}(\mathbf{y}) = g_{j,t}(\mathbf{y})$$

and can be split into two inequalities

$$\begin{cases} f_{j,t}(\mathbf{y}) \geq g_{j,t}(\mathbf{y}) & (3.1a) \\ f_{j,t}(\mathbf{y}) \leq g_{j,t}(\mathbf{y}) & (3.1b) \end{cases}$$

where we recognize that equation (3.1a) is the SOC constraint used in SOCP-OPF and where equation (3.1b) is in general a nonconvex constraint. To make equation (3.1b) convex, we linearize $g_{j,t}(\mathbf{y})$. Let $\bar{g}_{j,t}(\mathbf{y}, \mathbf{y}^k)$ be the linear approximation of $g_{j,t}(\mathbf{y})$ around \mathbf{y}^k , i.e.

$$\bar{g}_{j,t}(\mathbf{y}, \mathbf{y}^k) = g_{j,t}(\mathbf{y}^k) + \nabla g_{j,t}(\mathbf{y}^k)^\top (\mathbf{y} - \mathbf{y}^k)$$

We also add a slack variable $s_{j,t}$ to prevent the constraint to be too restrictive. Its role will be discussed in more details below. The slack variable is penalized in the objective to ensure convergence. Equation (3.1b) at iteration k becomes thus

$$f_{j,t}(\mathbf{y}) \leq s_{j,t} + \bar{g}_{j,t}(\mathbf{y}, \mathbf{y}^k)$$

Note that this constraint is convex. Let us also define the following notations :

- $\mathcal{Y}_{\text{SOCP}}$ is the set \mathcal{Y} where the nonconvex quadratic constraint has been relaxed to the corresponding SOC constraint. Recall that the quadratic constraints in \mathcal{Y} describe the border of some third order Lorentz cones. $\mathcal{Y}_{\text{SOCP}}$ is thus a superset of \mathcal{Y} in which the interior of the cones are added.
- \mathbf{z} is the vector of variables \mathbf{y} extended with $s_{j,t}$, i.e. $\mathbf{z} = \mathbf{y} \cup \{s_{j,t} \mid \forall j \in \mathcal{N}_+, \forall t \in \mathcal{T}\}$
- $\mathbf{c}_k^\top \mathbf{z}$ is the new cost at iteration k , i.e. $\mathbf{c}_k^\top \mathbf{z} = \mathbf{b}^\top \mathbf{y} + \rho^k (\sum_{j,t} s_{j,t})$ where ρ^k is a penalty parameter.
- \mathcal{Z}_k the feasible set for variables \mathbf{z} as

$$\mathcal{Z}_k = \left\{ \mathbf{z} = \mathbf{y} \cup \{s_{j,t}\} \mid \mathbf{y} \in \mathcal{Y}_{\text{SOCP}} \right. \\ \left. \begin{aligned} f_{j,t}(\mathbf{y}) &\leq s_{j,t} + \bar{g}_{j,t}(\mathbf{y}, \mathbf{y}^k), \quad \forall j \in \mathcal{N}_+, \forall t \in \mathcal{T} \\ s_{j,t} &\geq 0, \quad \forall j \in \mathcal{N}_+, \forall t \in \mathcal{T} \end{aligned} \right\}$$

With these notations, we can formally define the algorithm as follows :

Algorithm 1: The Convex-Concave Procedure for Feasibility Recovery.

Result: \mathbf{x}^* and \mathbf{z}^* feasible solution of (2.10)

Input: An initial penalty parameter ρ^1 ,
a penalty growth rate parameter τ ,
a penalty upper bound ρ_M ,
a feasibility tolerance ϵ .

Let $k = 1$;

Solve

$$\begin{aligned} \min_{\mathbf{x}, \mathbf{y}} \quad & \mathbf{a}^\top \mathbf{x} + \mathbf{b}^\top \mathbf{y} \\ \text{s.t.} \quad & \mathbf{x} \in \mathcal{X} \\ & (\mathbf{x}, \mathbf{y}) \in \mathcal{Y}_{\text{SOCP}}(\mathbf{d}) \end{aligned} \tag{3.2}$$

and let $(\mathbf{x}^1, \mathbf{y}^1)$ be the optimal solution ;

Gap $\leftarrow v_{j,t}^1 l_{j,t}^1 - (P_{j,t}^1)^2 + (Q_{j,t}^1)^2$;

while Gap $> \epsilon$ **do**

 Solve

$$\begin{aligned} \min_{\mathbf{x}, \mathbf{z}} \quad & \mathbf{a}^\top \mathbf{x} + \mathbf{c}_k^\top \mathbf{z} \\ \text{s.t.} \quad & \mathbf{x} \in \mathcal{X} \\ & (\mathbf{x}, \mathbf{z}) \in \mathcal{Z}_k(\mathbf{d}) \end{aligned} \tag{3.3}$$

 and let $(\mathbf{x}^{k+1}, \mathbf{z}^{k+1})$ be the optimal solution ;

 Gap $\leftarrow v_{j,t}^{k+1} l_{j,t}^{k+1} - (P_{j,t}^{k+1})^2 + (Q_{j,t}^{k+1})^2$;

$\rho^{k+1} = \min(\tau \rho^k, \rho_M)$;

$k \leftarrow k + 1$;

end

$\mathbf{x}^* \leftarrow \mathbf{x}^k$;

$\mathbf{z}^* \leftarrow \mathbf{z}^k$;

Note that in what follows, we will call this algorithm the Feasibility Recovery Procedure (FRP). Note also that problems (3.2) and (3.3) are both MISOCP and can thus be solved quite efficiently to optimality with existing solvers. Our goal is now to free the uncertain variables \mathbf{d} and solve (3.2) and (3.3) in a robust way with respect to \mathbf{d} . This is what is done in the next section (Section 2.6). Before, we show an example of the behavior of algorithm 1 on a simple problem.

Example

This example shows the behavior of the algorithm on a simple 3D problem and highlights the role of its parameters, namely ρ^1 and τ .

Suppose that we want to solve the following small example involving an SOC equality constraint :

$$\min_{x_1, x_2, x_3} x_1 \quad (3.4a)$$

$$\text{s.t. } x_1 = \sqrt{x_2^2 + x_3^2} \quad (3.4b)$$

$$x_1 \geq -x_2 + 1 \quad (3.4c)$$

$$x_1 \geq 0.5x_2 + 0.5 \quad (3.4d)$$

$$x_1 \geq -0.5x_3 + 1 \quad (3.4e)$$

$$x_1 \geq x_3 + 0.5 \quad (3.4f)$$

Note that if we ignore constraints (3.4c) to (3.4f), the solution is $x_1 = x_2 = x_3 = 0$ which would be the same solution as the corresponding SOCP relaxation. Constraints (3.4c) to (3.4f) are there to force the solution of the relaxation to be in the interior of the cone. Let's apply the FRP to obtain a sub-optimal but feasible solution. We first solve the following SOCP relaxation :

$$\min_{x_1, x_2, x_3} x_1 \quad (3.5a)$$

$$\text{s.t. } x_1 \geq \sqrt{x_2^2 + x_3^2} \quad (3.5b)$$

$$(3.4c) \text{ to } (3.4f)$$

The optimal solution is :

$$x^0 = [0.8333, 0.3513, 0.3333]$$

We can check that it violates constraint (3.4b). At iteration k , we solve :

$$\min_{x_1, x_2, x_3} x_1 + \rho^k s \quad (3.6a)$$

$$\text{s.t. } (3.5b), (3.4c) \text{ to } (3.4f)$$

$$x_1 \leq s + \sqrt{(x_2^k)^2 + (x_3^k)^2} + \frac{x_2^k}{\sqrt{(x_2^k)^2 + (x_3^k)^2}}(x_2 - x_2^k) + \frac{x_3^k}{\sqrt{(x_2^k)^2 + (x_3^k)^2}}(x_3 - x_3^k) \quad (3.6b)$$

Two views of the cut (3.6b) for $s = 0$ together with the cone (3.5b) for $k = 0$ are represented in Figure 3.1.

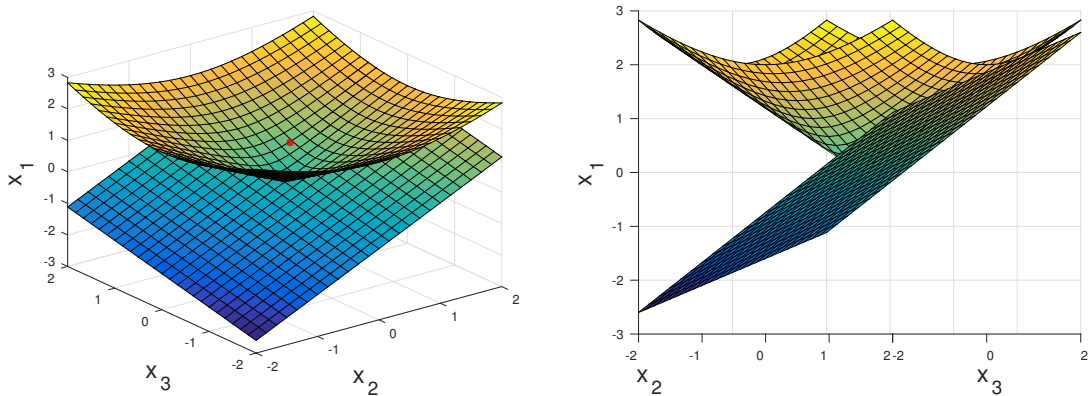


Figure 3.1: Two views of the cuts and the second order Lorentz cone. x^0 is represented by the red dot.

As Figure 3.1 gives us the intuition, equation (3.6b) forces the solution to lie on the extreme ray defined by $(\lambda\sqrt{(x_2^k)^2 + (x_3^k)^2}, \lambda x_2^k, \lambda x_3^k)$ for all $\lambda > 0$ when $s = 0$. The slack variable s controls how much the solution can deviate from this extreme ray. The role of ρ^1 and τ now appears clear : they will play on the rate at which we make s go to 0. For our example, we will show the iterations of the algorithm for two different choices of ρ^1 to show its role. We set $\tau = 2$.

First case : $\rho^1 = 0.5$ The iterations are given on table 3.1.

Iteration nb	Solution	ρ	s	gap
1	[0.8333, 0.6667, 0.3333]	0.5	0.1203	0.1389
2	[0.9045, 0.8090, 0.4045]	1	$8.7751 \cdot 10^{-9}$	$1.6029 \cdot 10^{-8}$

Table 3.1: Iterations of the FRP for $\rho^1 = 0.5$

On the following figure, we show these iterations on the level curves of the cone, together with the associated extreme ray.

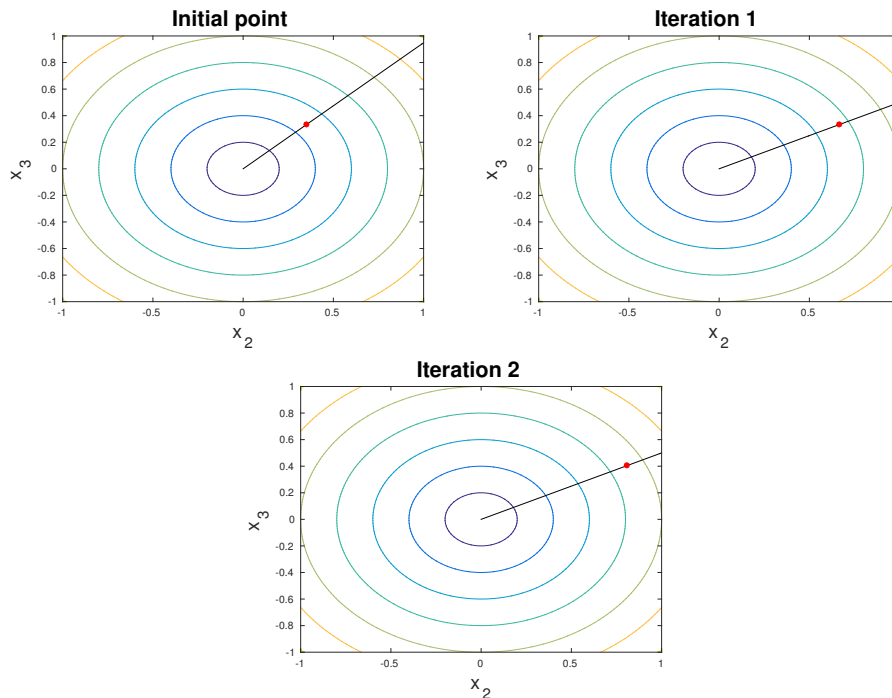


Figure 3.2: Representation of the iterations (in red) on the level curves of the cone. The black line represents the corresponding extreme ray.

We can see that as ρ^1 is rather small, the first solution found has a nonzero s and is not on the same extreme ray as the projection of the previous solution x^0 on the cone. At the next iteration, ρ increases, which makes s go to zero and consequently the solution lies on the same extreme ray as the projection of x^1 . This makes also the gap go to zero.

Second case : $\rho^1 = 100$ The table of iterations becomes

Iteration nb	Solution	ρ	s	gap
1	[1.5211, 1.1274, 1.0211]	100	$4.0733 \cdot 10^{-4}$	$9.8959 \cdot 10^{-11}$

Table 3.2: Iterations of the FRP for $\rho^1 = 0.5$

Now, as ρ^1 is large, the optimal solution will be to directly have $s = 0$. The optimal solution is thus the feasible solution with the smallest cost that lies on the same extreme ray as the projection of x^0 . Note that obviously, the final solution in this second case has a larger cost than the solution obtained in the first case. However, it converged in fewer iterations.

In conclusion, this example shows that it is important to pick an initial penalty parameter that is not too large in order to prevent the difference between two successive solutions to be too large. The price to pay is a greater number of iterations.

3.2 Two-stage algorithm

In this section, I will focus on problem (3.3) and show, based on [4], how we can solve its robust counterpart. The same procedure can be applied to problem (3.2). We thus wish to solve

$$\min_{x \in \mathcal{X}} \left(\mathbf{a}^\top \mathbf{x} + \max_{\mathbf{d} \in \mathcal{D}} \min_{z \in \mathcal{Z}_k(\mathbf{x}, \mathbf{d})} \mathbf{c}_k^\top \mathbf{z} \right) \quad (3.7)$$

where \mathbf{d} is now considered as variable. Notice that problem (3.7) can be equivalently reformulated as

$$\begin{aligned} \min_{x \in \mathcal{X}, \eta} \quad & \mathbf{a}^\top \mathbf{x} + \eta \\ \text{s.t.} \quad & \eta \geq \min_{z \in \mathcal{Z}_k(\mathbf{x}, \mathbf{d})} \mathbf{c}_k^\top \mathbf{z}, \quad \mathbf{d} \in \mathcal{D} \end{aligned}$$

Then, by adding one variable $\mathbf{z}(\mathbf{d})$ for each possible value of the uncertain variable \mathbf{d} , we can formulate the same problem as

$$\begin{aligned} \min_{x \in \mathcal{X}, \eta, \mathbf{z}(\cdot)} \quad & \mathbf{a}^\top \mathbf{x} + \eta \\ \text{s.t.} \quad & \eta \geq \mathbf{c}_k^\top \mathbf{z}(\mathbf{d}), \quad \mathbf{d} \in \mathcal{D} \\ & \mathbf{z}(\mathbf{d}) \in \mathcal{Z}_k(\mathbf{x}, \mathbf{d}), \quad \mathbf{d} \in \mathcal{D} \end{aligned}$$

At the optimum, the value of $\mathbf{z}(\mathbf{d})$ will be the one associated to the worst case. Therefore, if we had a way to find the worst case of the uncertainty $\mathbf{d}_{\text{worst}}$ in advance, the problem to solve would simply be

$$\begin{aligned} \min_{x \in \mathcal{X}, \eta, \mathbf{d}_{\text{worst}}} \quad & \mathbf{a}^\top \mathbf{x} + \eta \\ \text{s.t.} \quad & \eta \geq \mathbf{c}_k^\top \mathbf{z}(\mathbf{d}_{\text{worst}}) \\ & \mathbf{z}(\mathbf{d}_{\text{worst}}) \in \mathcal{Z}_k(\mathbf{x}, \mathbf{d}_{\text{worst}}) \end{aligned}$$

which is an MISOCP problem for which there exists efficient solvers. The idea of Lorca and Sun's algorithm will thus be to include only a subset of all the $\mathbf{z}(\mathbf{d})$ variables and design a strategy to try to find the worst case as soon as possible.

Their suggestion is to use a two-stage solution strategy. Let $\mathcal{S} = \{\mathbf{d}_1^*, \dots, \mathbf{d}_k^*\}$ be the worst case candidates found so far, with all the $\mathbf{d}_j^* \in \mathcal{D}$.

At the k_{th} iteration, we first solve the following master problem :

$$\begin{aligned} \min_{\mathbf{x} \in \mathcal{X}, \eta, \mathbf{y}(\cdot)} \quad & \mathbf{a}^\top \mathbf{x} + \eta \\ \text{s.t.} \quad & \eta \geq \mathbf{c}_k^\top \mathbf{z}(\mathbf{d}), \quad \mathbf{d} \in \mathcal{S} \\ & \mathbf{z}(\mathbf{d}) \in \mathcal{Z}_k(\mathbf{x}, \mathbf{d}), \quad \mathbf{d} \in \mathcal{S} \end{aligned}$$

to obtain a first-stage solution \mathbf{x} . We then solve the following second-stage problem, also called the slave :

$$Q(\mathbf{x}) = \max_{\mathbf{d} \in \mathcal{D}} \min_{\mathbf{z}_k \in \mathcal{Z}_k(\mathbf{x}, \mathbf{d})} \mathbf{c}_k^\top \mathbf{z}$$

to obtain the new worst-case realization of uncertainty \mathbf{d}_{k+1}^* corresponding to the fixed investment \mathbf{x} . Notice that if the worst case has already been discovered and is contained in \mathcal{S} , then $\eta \geq Q(\mathbf{x})$ necessarily holds. Indeed, the second stage minimize $\mathbf{c}_k^\top \mathbf{z}$ subject to the worst case but doesn't see the first stage cost $\mathbf{a}^\top \mathbf{x}$. It will thus always do better. Therefore, if $Q(\mathbf{x}) > \eta$, it necessarily means that we have not found the worst case yet. Thus, we update \mathcal{S} as $\mathcal{S} \cup \{\mathbf{d}_{k+1}^*\}$ and proceed to a new iteration. Otherwise, the algorithm terminates. It is proven in [4] that the algorithm converges in a finite number of steps.

The interactions between the master and the slave are represented schematically in the following figure :

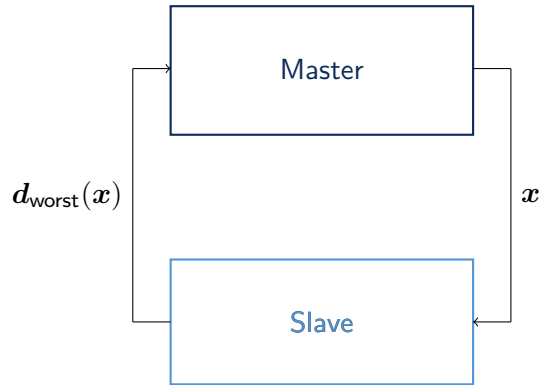


Figure 3.3: Master-Slave interactions

3.2.1 First-stage solution

Recall that at iteration k , we have to solve the following master problem :

$$\begin{aligned} \min_{\mathbf{x} \in \mathcal{X}} \quad & \mathbf{a}^\top \mathbf{x} + \eta \\ \text{s.t.} \quad & \eta \geq \mathbf{c}_k^\top \mathbf{z}(\mathbf{d}), \quad \mathbf{d} \in \mathcal{S} \\ & \mathbf{z}(\mathbf{d}) \in \mathcal{Z}_k(\mathbf{x}, \mathbf{d}), \quad \mathbf{d} \in \mathcal{S} \end{aligned}$$

Note that this problem belongs to the class of MISOCP. Indeed, \mathcal{Y} is a set of linear and SOC constraints and \mathcal{X} contains integer restrictions constraints.

3.2.2 Second-stage solution

The problem to solve at the second stage is

$$\max_{d \in \mathcal{D}} \min_{z_k \in \mathcal{Z}_k(x, d)} \mathbf{c}_k^\top z \quad (3.8)$$

As $\mathcal{Z}_k(x, d)$ is a conic set, there exists a matrix A , a matrix G , a matrix H , a vector f and a cone \mathcal{K} such that

$$\mathcal{Z}_k(x, d) = \{z | Az \geq_{\mathcal{K}} Gx + Hd + f\}$$

where the notation $x \geq_{\mathcal{K}} y$ used in conic theory means that $x - y \in \mathcal{K}$. In our case, the cone \mathcal{K} is the cartesian product of a nonnegative orthant cone and a Lorentz cone.

We now notice that, by using the conic duality theory, problem (3.8) is equivalent to the following bi-conic problem :

$$\max_{\pi, d} \{\pi^\top (f + Gx) + \pi^\top Hd : d \in \mathcal{D}, \pi^\top A = \mathbf{b}^\top, \pi \geq_{\mathcal{K}} 0\} \quad (3.9)$$

This can be solved by the alternating direction method which consists in fixing sequentially π and d and solving the following two conic problems

$$\max_{\pi} \{\pi^\top (f + Gx) + \pi^\top Hd : \pi^\top A = \mathbf{b}^\top, \pi \geq_{\mathcal{K}} 0\}$$

$$\max_d \{\pi^\top (f + Gx) + \pi^\top Hd : d \in \mathcal{D}\}$$

until convergence, that is, until their respective objective function coincides. Note that the finite convergence can also be proven for this problem [4].

It remains now to show how we can obtain the value of C_f that will lead to the right amount of unplanned curtailment. This is what is done in the next section.

3.3 How to find C_f ?

We argued in section 2.2 that by playing with the cost of fuse C_f we can reach a value of unplanned curtailment that is much reduced compared to the value obtained without fuse limits. In this section, we will describe a systematic method to find this value C_f .

We first define the following function :

$$\text{Fuse} : [0, \infty] \rightarrow [-0.1, 0.9] : \text{Fuse}(C_f) \rightarrow x_{\text{unplanned}}^{\%} - 0.1$$

with $x_{i,t}^+$ and $x_{i,t}^-$ solution of algorithm 1 with equations (3.2) and (3.3) replaced by their robust counterparts and with C_f fixed. Our goal is to find a root of this function. Note that we do not know anything about the analytic expression of the function but we can evaluate it in any point by solving model (2). A method to find the root of a nonlinear continuous function is the bisection method.

This method is described in the following algorithm :

Algorithm 2: The bisection algorithm to find C_f

Result: C_f such that $x_{\text{unplanned}}^{\%} = 0.1$
Input: \overline{C}_f and \underline{C}_f such that $\text{Fuse}(\overline{C}_f)\text{Fuse}(\underline{C}_f) < 0$
 $C_f = \frac{\overline{C}_f + \underline{C}_f}{2}$;
while $\text{Fuse}(C_f) \neq 0$ **do**
 if $\text{Fuse}(C_f)\text{Fuse}(\underline{C}_f) > 0$ **then**
 | $\underline{C}_f \leftarrow C_f$;
 else
 | $\overline{C}_f \leftarrow C_f$;
 end
 $C_f = \frac{\overline{C}_f + \underline{C}_f}{2}$;
end

In practice, we will allow a tolerance for convergence. That is, the algorithm will terminate if $x_{\text{unplanned}}$ is between $0.1 - \text{tol}$ and $0.1 + \text{tol}$, where tol is the fixed tolerance.

3.4 Dual problem

In view of equation (3.9), we need to derive the conic dual of problems (3.2) and (3.3). This is what we will do in this section. We will also comment on the interpretation that we can make of the dual variables and constraints.

Before deriving the whole dual, let us first discuss the specific case of the dual of the SOCP-OPF equations presented in section 2.1. The dual of these equations are indeed of particular interest as they give insight on the value of electricity in the grid. Moreover, to the best of our knowledge, this work is the first to use the conic dual of the SOCP formulation to derive an expression of the locational marginal prices of electricity.

3.4.1 Distribution Locational Marginal Prices

As explained in [1], many DERs have locational value, that is, their value depends on their location. The electrical energy is one of them. The locational nature of the value of electricity is due to network constraints and losses. In the same way, this value has also a temporal nature due to the dependence in time of the demand and the production. Moreover, these differences in location and time exacerbates with the fact the the system is becoming more distributed. In this context, it can be interesting to price electricity differently depending on the location and the time of the day at which the consumption occurs. This is called nodal pricing and is used in the United States, among others. The prices of electricity in the nodal pricing market design are called Locational Marginal Prices (LMP). Whereas they can be easily calculated for high-voltage systems using the dual of the Direct Current Optimal Power Flow (DCOPF) equations, it is much more challenging to compute them in low-voltage systems such as distribution networks as the equations are nonlinear and in general not even convex. However, we can use the SOCP relaxation presented in equations (2.2) and the conic duality theory to get insights about LMPs in distribution networks.

In this section, we wish to investigate the evolution of the LMP in a simple network and derive an expression for this evolution. We will thus formulate the constraints when the network is a path graph

and derive the dual of the AC-OPF constraints for this simple network. From these equations, we will derive a fundamental expression for the evolution of the LMP and then analyze this result.

Primal formulation

We consider throughout this analysis that the graph underlying the network is a path graph. In that case, a simpler formulation of the single stage SOCP-OPF problem along with the dual variables of the constraint can be written as:

$$\begin{aligned}
& \min_{q,P,Q,v,l} \sum_{j=1}^n r_j l_j \\
\text{s.t. } & (\pi_{a,0}) : 0 = p_0 + P_1 - r_1 l_1 \\
& (\pi_{r,0}) : 0 = q_0 + Q_1 - x_1 l_1 \\
& (\pi_{v,i}) : v_{i-1} = v_i - 2(r_i P_i + x_i Q_i) + (r_i^2 + x_i^2) l_i, \quad \forall i \in \mathcal{N}_+ \\
& (\pi_{a,i}) : P_i = p_i + P_{i+1} - r_{i+1} l_{i+1}, \quad \forall i \in \{1, n-1\} \\
& (\pi_{r,i}) : Q_i = q_i + Q_{i+1} - x_{i+1} l_{i+1}, \quad \forall i \in \{1, n-1\} \\
& (\pi_{a,n}) : P_n = p_n \\
& (\pi_{r,n}) : Q_n = q_n \\
& (\sigma_i^+) : v_i \leq \bar{v}_i, \quad \forall i \in \mathcal{N}_+ \\
& (\sigma_i^-) : v_i \geq \underline{v}_i, \quad \forall i \in \mathcal{N} \\
& (\eta_i^+) : l_i \leq \bar{l}_i, \quad \forall i \in \mathcal{N}_+ \\
& (\eta_i^-) : l_i \geq 0, \quad \forall i \in \mathcal{N}_+ \\
& \begin{pmatrix} \gamma_{i1} \\ \gamma_{i2} \\ \gamma_{i3} \\ \gamma_{i4} \end{pmatrix} : \begin{pmatrix} v_i + l_i \\ v_i - l_i \\ 2P_i \\ 2Q_i \end{pmatrix} \in \mathbb{L}^3, \quad \forall i \in \{1, n\}
\end{aligned}$$

Dual formulation

For this formulation, the dual can be written as :

$$\max_{\pi, \sigma, \eta, \gamma} \sum_{i \in \mathcal{N}_+} (-\eta_i \bar{l}) + \sum_{i \in \mathcal{N}} (\sigma_i^- \underline{v} - \sigma_i^+ \bar{v}) \quad (3.10a)$$

$$\text{s.t. } (v_0) : \pi_{v,1} + \sigma_0^+ - \sigma_0^- = 0 \quad (3.10b)$$

$$(v_i) : \pi_{v,i} - \pi_{v,i+1} - \gamma_{i1} - \gamma_{i2} + \sigma_i^+ - \sigma_i^- = 0, \quad \forall i \in \{1, n-1\} \quad (3.10c)$$

$$(v_n) : \pi_{v,n} - \gamma_{n1} - \gamma_{n2} + \sigma_n^+ - \sigma_n^- = 0 \quad (3.10d)$$

$$(l_i) : (x_i^2 + r_i^2) \pi_{v,i} - r_i \pi_{a,i-1} - x_i \pi_{r,i-1} - \gamma_{i1} + \gamma_{i2} + \eta_i^+ = -r_i, \quad \forall i \in \{1, n\} \quad (3.10e)$$

$$(P_i) : -2r_i \pi_{v,i} - \pi_{a,i} + \pi_{a,i-1} - 2\gamma_{i3} = 0, \quad \forall i \in \{1, n\} \quad (3.10f)$$

$$(Q_i) : -2x_i \pi_{v,i} - \pi_{r,i} + \pi_{r,i-1} - 2\gamma_{i4} = 0, \quad \forall i \in \{1, n\} \quad (3.10g)$$

$$(q_i) : \pi_{r,i} = 0 \quad (3.10h)$$

$$\begin{pmatrix} \gamma_{i1} \\ \gamma_{i2} \\ \gamma_{i3} \\ \gamma_{i4} \end{pmatrix} \in \mathbb{L}^3, \quad \forall i \in \{1, n\} \quad (3.10i)$$

To simplify the analysis, we consider that voltage and current limits are not binding, which implies that the corresponding dual variables σ and η take the value 0. By combining equations (3.10b) to (3.10i), we can eliminate variables γ 's that are hard to interpret and obtain the evolution of the active power price at node i in terms of prices at its neighbors :

$$\begin{aligned} \pi_{a,i-1} = \frac{-F \pm \sqrt{F^2 - 4E}}{2} &= \pi_{a,i} + 2r_i \pi_{v,i+1} \\ &\pm 2\sqrt{r_i^2 \pi_{v,i} (\pi_{v,i+1} - \pi_{v,i}) + r_i \pi_{a,i} (\pi_{v,i+1} - \pi_{v,i}) - r_i (\pi_{v,i+1} - \pi_{v,i})} \end{aligned} \quad (3.11)$$

The details of the computations are provided in appendix A. With this equation, we can see that the active power price at one node depends on the price at the following node as well as on the price of voltage at the two next nodes.

Equation (3.11) represents two solutions, depending on whether the power is produced ($p_{i,t}$ is positive) or consumed ($p_{i,t}$ is negative) at node i .

Graphs representing the evolution of prices (power and voltage) and attesting the validity of equation (3.11) are also given in appendix A.

3.4.2 Dual of the complete problem

Problem (3.2) together with dual variables for constraints involving second stage variables is given in model 6. Model 7 gives the corresponding dual. Problem (3.3) and its dual are given in models 8

and 9.

Model 6 Primal ODP (Primal-ODP)

Minimize:

$$C_f(\bar{K} - \underline{K}) + \sum_{g,j} (w_g \bar{L}_j C_g) + C_s \sum_{i,t} f_i + \eta \quad (3.12a)$$

Subject to:

$$\eta \geq C_+ \left(\sum_{i,t} x_{i,t}^+ \right) + VOLL \left(\sum_{i,t} x_{i,t}^- \right) + \sum_{g,j} \left(\bar{L}_j r_g \tilde{l}_{j,t,g} \right) \quad (3.12b)$$

$$\sum_{g \in \mathcal{G}} w_g = 1$$

w_g binary

$$(\pi_{a,0,t}) : p_{0,t}^{in} - p_{0,t}^{out} = p_{0,t} + \sum_{j \in \mathcal{C}_0} \left(P_{j,t} - \left(\sum_{g \in \mathcal{G}} \bar{L}_j r_g \tilde{l}_{j,t,g} \right) \right), \quad \forall t \in \mathcal{T} \quad (3.12c)$$

$$(\pi_{r,0,t}) : 0 = q_{0,t} + \sum_{j \in \mathcal{C}_0} \left(Q_{j,t} - \left(\sum_{g \in \mathcal{G}} \bar{L}_j x_g \tilde{l}_{j,t,g} \right) \right), \quad \forall t \in \mathcal{T} \quad (3.12d)$$

$$(\pi_{v,i,t}) : v_{\mathcal{A}_i,t} = v_{i,t} - 2 \left(\sum_{g \in \mathcal{G}} \bar{L}_i r_g \tilde{P}_{i,t,g} + \bar{L}_i x_g \tilde{Q}_{i,t,g} + \bar{L}_i^2 (r_g^2 + x_g^2) \tilde{l}_{i,t,g} \right), \quad (3.12e)$$

$$\forall i \in \mathcal{N}_+, \quad \forall t \in \mathcal{T}$$

$$(\pi_{a,i,t}) : P_{i,t} + p_{i,t}^{in} - p_{i,t}^{out} = p_{i,t} + \sum_{j \in \mathcal{C}_i} \left(P_{j,t} - \left(\sum_{g \in \mathcal{G}} \bar{L}_j r_g \tilde{l}_{j,t,g} \right) \right), \quad \forall i \in \mathcal{N}_+, \quad \forall t \in \mathcal{T} \quad (3.12f)$$

$$(\pi_{r,i,t}) : Q_{i,t} = q_{i,t} + \sum_{j \in \mathcal{C}_i} \left(Q_{j,t} - \left(\sum_{g \in \mathcal{G}} \bar{L}_j x_g \tilde{l}_{j,t,g} \right) \right), \quad \forall i \in \mathcal{N}_+, \quad \forall t \in \mathcal{T} \quad (3.12g)$$

$$\begin{pmatrix} \gamma_{i1,t} \\ \gamma_{i2,t} \\ \gamma_{i3,t} \\ \gamma_{i4,t} \end{pmatrix} : \begin{pmatrix} v_{i,t} + l_{i,t} \\ v_{i,t} - l_{i,t} \\ 2P_{i,t} \\ 2Q_{i,t} \end{pmatrix} \in \mathbb{L}^3, \quad \forall i \in \mathcal{N}_+, \quad \forall t \in \mathcal{T} \quad (3.12h)$$

$$(\sigma_{i,t}^-, \sigma_{i,t}^+) : \underline{v} \leq v_{i,t} \leq \bar{v}, \quad \forall i \in \mathcal{N}, \quad \forall t \in \mathcal{T} \quad (3.12i)$$

$$(\kappa_{i,t}^-, \kappa_{i,t}^+) : \underline{K} \leq p_{i,t} \leq \bar{K}, \quad \forall i \in \mathcal{N}_+, \quad \forall t \in \mathcal{T} \quad (3.12j)$$

$$(\zeta_{i,t}) : d_{i,t} - x_{i,t}^+ + x_{i,t}^- = p_{i,t}, \quad \forall i \in \mathcal{N}_+, \quad \forall t \in \mathcal{T} \quad (3.12k)$$

$$(\chi_{i,t}^+) : x_{i,t}^+ \geq 0, \quad \forall i \in \mathcal{N}_+, \quad \forall t \in \mathcal{T} \quad (3.12l)$$

$$(\chi_{i,t}^-) : x_{i,t}^- \geq 0, \quad \forall i \in \mathcal{N}_+, \quad \forall t \in \mathcal{T} \quad (3.12m)$$

$$(\eta_{i,t}^-, \eta_{i,t}^+) : 0 \leq l_{i,t} \leq \sum_{g \in \mathcal{G}} w_g I_g, \quad \forall i \in \mathcal{N}_+, \quad \forall t \in \mathcal{T} \quad (3.12n)$$

$$(\varpi_{1,j,t,g}^-, \varpi_{1,j,t,g}^+) : \underline{P} w_g \leq \tilde{P}_{j,t,g} \leq \bar{P} w_g, \quad \forall j \in \mathcal{N}_+, \quad \forall t \in \mathcal{T}, \quad \forall g \in \mathcal{G} \quad (3.12o)$$

$$(\varpi_{2,j,t,g}^-, \varpi_{2,j,t,g}^+) : P_{j,t} - (1 - w_g) \bar{P} \leq \tilde{P}_{j,t,g} \leq P_{j,t} - (1 - w_g) \underline{P}, \quad \forall j \in \mathcal{N}_+, \quad \forall t \in \mathcal{T}, \quad \forall g \in \mathcal{G} \quad (3.12p)$$

$$(\rho_{1,j,t,g}^-, \rho_{1,j,t,g}^+) : \underline{Q}w_g \leq \tilde{Q}_{j,t,g} \leq \overline{Q}w_g, \quad \forall j \in \mathcal{N}_+, \forall t \in \mathcal{T}, \forall g \in \mathcal{G} \quad (3.12q)$$

$$(\rho_{2,j,t,g}^-, \rho_{2,j,t,g}^+) : \underline{Q}_{j,t} - (1 - w_g)\overline{Q} \leq \tilde{Q}_{j,t,g} \leq \underline{Q}_{j,t} - (1 - w_g)\underline{Q}, \quad \forall j \in \mathcal{N}_+, \forall t \in \mathcal{T}, \forall g \in \mathcal{G} \quad (3.12r)$$

$$(\iota_{1,j,t,g}^-, \iota_{1,j,t,g}^+) : 0 \leq \tilde{l}_{j,t,g} \leq I_{N_{\text{choices}}}w_g, \quad \forall j \in \mathcal{N}_+, \forall t \in \mathcal{T}, \forall g \in \mathcal{G} \quad (3.12s)$$

$$(\iota_{2,j,t,g}^-, \iota_{2,j,t,g}^+) : l_{j,t} - (1 - w_g)I_{N_{\text{choices}}} \leq \tilde{l}_{j,t,g} \leq l_{j,t}, \quad \forall j \in \mathcal{N}_+, \forall t \in \mathcal{T}, \forall g \in \mathcal{G} \quad (3.12t)$$

$$(\tau_{i,t}^-, \tau_{i,t}^+) : 0 \leq e_{i,t} \leq f_i, \quad \forall i \in \mathcal{N}, \forall t \in \mathcal{T} \quad (3.12u)$$

$$(\delta_{i,t}^{in-}, \delta_{i,t}^{in+}) : \underline{p}_i^{in} \leq p_{i,t}^{in} \leq \overline{p}_i^{in}, \quad \forall i \in \mathcal{N}, \forall t \in \mathcal{T} \quad (3.12v)$$

$$(\delta_{i,t}^{out-}, \delta_{i,t}^{out+}) : \underline{p}_i^{out} \leq p_{i,t}^{out} \leq \overline{p}_i^{out}, \quad \forall i \in \mathcal{N}, \forall t \in \mathcal{T} \quad (3.12w)$$

$$(\nu_{i,t}) : e_{i,t} = e_{i,t-1} + h \left(\xi_{in} p_{i,t-1}^{in} - \frac{1}{\xi_{out}} p_{i,t-1}^{out} \right), \quad \forall i \in \mathcal{N}, \forall t \in \mathcal{T}_+ \quad (3.12x)$$

$$(\nu_{i,1}) : e_{i,1} = 0, \quad \forall i \in \mathcal{N} \quad (3.12y)$$

Model 7 Dual ODP (Dual-ODP)

Maximize:

$$\begin{aligned} & - \sum_{i,t} \left(\sigma_{i,t}^+ \overline{v} - \sigma_{i,t}^- \underline{v} - \zeta_{i,t} d_{i,t} + \tau_{i,t}^+ f_i + \delta_{i,t}^{in,+} \overline{p}_i^{in} - \delta_{i,t}^{in,-} \underline{p}_i^{in} + \delta_{i,t}^{out,+} \overline{p}_i^{out} - \delta_{i,t}^{out,-} \underline{p}_i^{out} \right) \\ & - \sum_{j,t,g} \left(\varpi_{1,j,t,g}^+ \overline{P}w_g - \varpi_{1,j,t,g}^- \underline{P}w_g - \varpi_{2,j,t,g}^+ \underline{P}(1 - w_g) + \varpi_{2,j,t,g}^- \overline{P}(1 - w_g) + \rho_{1,j,t,g}^+ \overline{Q}w_g \right. \\ & - \rho_{1,j,t,g}^- \underline{Q}w_g - \rho_{2,j,t,g}^+ \underline{Q}(1 - w_g) + \rho_{2,j,t,g}^- \overline{Q}(1 - w_g) + \iota_{1,j,t,g}^+ I_{N_{\text{choices}}}w_g \\ & \left. + \iota_{2,j,t,g}^- (1 - w_g) I_{N_{\text{choices}}} \right) - \sum_{j,t} \left(\kappa_{j,t}^+ \overline{K} - \kappa_{j,t}^- \underline{K} + \eta_{j,t}^+ \left(\sum_g w_g I_g \right) \right) \end{aligned} \quad (3.13a)$$

$$(3.13b)$$

Subject to:

$$(P_{i,t}) : \pi_{a,i,t} - \pi_{a,A_i,t} - 2\gamma_{i3,t} + \sum_g \left(\varpi_{2,i,t,g}^- - \varpi_{2,i,t,g}^+ \right) = 0, \quad \forall i \in \mathcal{N}_+, \forall t \in \mathcal{T} \quad (3.13c)$$

$$(Q_{i,t}) : \pi_{r,i,t} - \pi_{r,A_i,t} - 2\gamma_{i4,t} + \sum_g \left(\rho_{2,i,t,g}^- - \rho_{2,i,t,g}^+ \right) = 0, \quad \forall i \in \mathcal{N}_+, \forall t \in \mathcal{T} \quad (3.13d)$$

$$(p_{i,t}) : -\pi_{a,i,t} + \kappa_{i,t}^+ - \kappa_{i,t}^- - \zeta_{i,t} = 0, \quad \forall i \in \mathcal{N}_+, \forall t \in \mathcal{T} \quad (3.13e)$$

$$(p_{0,t}) : -\pi_{a,0,t} = 0, \quad \forall t \in \mathcal{T} \quad (3.13f)$$

$$(q_{i,t}) : -\pi_{r,i,t} = 0, \quad \forall i \in \mathcal{N}, \forall t \in \mathcal{T} \quad (3.13g)$$

$$(v_{i,t}) : -\pi_{v,i,t} + \sum_{j \in \mathcal{C}_i} \pi_{v,j,t} - \gamma_{i1,t} - \gamma_{i2,t} + \sigma_{i,t}^+ - \sigma_{i,t}^- = 0, \quad \forall i \in \mathcal{N}_+, \forall t \in \mathcal{T} \quad (3.13h)$$

$$(v_{0,t}) : \sum_{j \in \mathcal{C}_0} \pi_{v,j,t} + \sigma_{0,t}^+ - \sigma_{0,t}^- = 0, \quad \forall t \in \mathcal{T} \quad (3.13i)$$

$$(l_{i,t}) : \sum_g \left(l_{2,i,t,g}^- - l_{2,i,t,g}^+ \right) - \gamma_{i1,t} + \gamma_{i2,t} + \eta_{i,t}^+ - \eta_{i,t}^- = 0, \quad \forall i \in \mathcal{N}_+, \quad \forall t \in \mathcal{T} \quad (3.13j)$$

$$(e_{i,t}) : \tau_{i,t}^+ - \tau_{i,t}^- + \nu_{i,t} - \nu_{i,t+1} = 0, \quad \forall i \in \mathcal{N}, \quad \forall t \in \mathcal{T}_- \quad (3.13k)$$

$$(e_{i,T}) : \tau_{i,T}^+ - \tau_{i,T}^- + \nu_{i,T} = 0, \quad \forall i \in \mathcal{N} \quad (3.13l)$$

$$(p_{i,t}^{in}) : \pi_{a,i,t} + \delta_{i,t}^{in,+} - \delta_{i,t}^{in,-} - h \xi_{in} \nu_{i,t+1} = 0, \quad \forall i \in \mathcal{N}, \quad \forall t \in \mathcal{T}_- \quad (3.13m)$$

$$(p_{i,t}^{out}) : -\pi_{a,i,t} + \delta_{i,t}^{out,+} - \delta_{i,t}^{out,-} + \frac{h}{\xi_{out}} \nu_{i,t+1} = 0, \quad \forall i \in \mathcal{N}, \quad \forall t \in \mathcal{T}_- \quad (3.13n)$$

$$(p_{i,T}^{in}) : \pi_{a,i,T} + \delta_{i,T}^{in,+} - \delta_{i,T}^{in,-} = 0, \quad \forall i \in \mathcal{N} \quad (3.13o)$$

$$(p_{i,T}^{out}) : -\pi_{a,i,T} + \delta_{i,T}^{out,+} - \delta_{i,T}^{out,-} = 0, \quad \forall i \in \mathcal{N} \quad (3.13p)$$

$$(x_{i,t}^+) : -\zeta_{i,t} - \chi_{i,t}^+ = -C_+, \quad \forall i \in \mathcal{N}_+, \quad \forall t \in \mathcal{T} \quad (3.13q)$$

$$(x_{i,t}^-) : \zeta_{i,t} - \chi_{i,t}^- = -VOLL, \quad \forall i \in \mathcal{N}_+, \quad \forall t \in \mathcal{T} \quad (3.13r)$$

$$(\tilde{P}_{j,t,g}) : 2\bar{L}_j r_g \pi_{v,j,t} + \varpi_{1,j,t,g}^+ - \varpi_{1,j,t,g}^- + \varpi_{2,j,t,g}^+ - \varpi_{2,j,t,g}^- = 0, \quad \forall j \in \mathcal{N}_+, \quad \forall t \in \mathcal{T}, \quad \forall g \in \mathcal{G} \quad (3.13s)$$

$$(\tilde{Q}_{j,t,g}) : 2\bar{L}_j x_g \pi_{v,j,t} + \rho_{1,j,t,g}^+ - \rho_{1,j,t,g}^- + \rho_{2,j,t,g}^+ - \rho_{2,j,t,g}^- = 0, \quad \forall j \in \mathcal{N}_+, \quad \forall t \in \mathcal{T}, \quad \forall g \in \mathcal{G} \quad (3.13t)$$

$$(\tilde{l}_{j,t,g}) : \bar{L}_j r_g \pi_{a,A_j,t} + \bar{L}_j x_g \pi_{r,A_j,t} + 2\bar{L}_j^2 (r_g^2 + x_g^2) \pi_{v,j,t} + l_{1,j,t,g}^+ - l_{1,j,t,g}^- + l_{2,j,t,g}^+ - l_{2,j,t,g}^- = -\bar{L}_j r_g, \quad \forall j \in \mathcal{N}_+, \quad \forall t \in \mathcal{T}, \quad \forall g \in \mathcal{G} \quad (3.13u)$$

$$\sigma_{i,t}^+, \sigma_{i,t}^-, \kappa_{i,t}^+, \kappa_{i,t}^-, \chi_{i,t}^+, \chi_{i,t}^-, \eta_{j,t}^+, \eta_{j,t}^-, \varpi_{1,j,t,g}^+, \varpi_{1,j,t,g}^-, \varpi_{2,j,t,g}^+, \varpi_{2,j,t,g}^-, \rho_{1,j,t,g}^+, \rho_{1,j,t,g}^-, \rho_{2,j,t,g}^+, \rho_{2,j,t,g}^-, l_{1,j,t,g}^+, l_{1,j,t,g}^-, l_{2,j,t,g}^+, l_{2,j,t,g}^-, \tau_{i,t}^+, \tau_{i,t}^-, \delta_{i,t}^{in,+}, \delta_{i,t}^{in,-}, \delta_{i,t}^{out,+}, \delta_{i,t}^{out,-}, \zeta_{0,t} \geq 0 \quad (3.13v)$$

$$\begin{pmatrix} \gamma_{i1,t} \\ \gamma_{i2,t} \\ \gamma_{i3,t} \\ \gamma_{i4,t} \end{pmatrix} \in \mathbb{L}^3, \quad \forall i \in \mathcal{N}_+, \quad \forall t \in \mathcal{T} \quad (3.13w)$$

Model 8 Primal Feasibility Recovery ODP (Primal-FR-ODP)

Minimize:

$$(3.12a)$$

Subject to:

$$\eta \geq VOLL\left(\sum_{i,t} x_{i,t}^+ + x_{i,t}^-\right) + \sum_{g,j} \left(\bar{L}_j r_g \tilde{l}_{j,t,g}\right) + \rho\left(\sum_{j,t} s_{j,t}\right) \quad (3.14a)$$

(3.12c) to (3.12y)

$$\begin{pmatrix} \gamma_{i5,t} \\ \gamma_{i6,t} \\ \gamma_{i7,t} \end{pmatrix} : \begin{pmatrix} f_{j,t} + 1 \\ f_{j,t} - 1 \\ 2v_{j,t} + 2l_{j,t} \end{pmatrix} \in \mathbb{L}^3, \quad \forall j \in \mathcal{N}_+, \forall t \in \mathcal{T} \quad (3.14b)$$

$$\begin{aligned} (\lambda_{j,t}) : & f_{j,t} = s_{j,t} + (v_{j,t}^k - l_{j,t}^k)^2 + (2P_{j,t}^k)^2 + (2Q_{j,t}^k)^2 \\ & + 2(v_{j,t}^k - l_{j,t}^k)(v_{j,t} - v_{j,t}^k) - 2(v_{j,t}^k - l_{j,t}^k)(l_{j,t} - l_{j,t}^k) \\ & + 8P_{j,t}^k(P_{j,t} - P_{j,t}^k) + 8Q_{j,t}^k(Q_{j,t} - Q_{j,t}^k), \quad \forall j \in \mathcal{N}_+, \forall t \in \mathcal{T} \end{aligned} \quad (3.14c)$$

$$(v_{j,t}) : s_{j,t} \geq 0, \quad \forall j \in \mathcal{N}_+, \forall t \in \mathcal{T} \quad (3.14d)$$

Model 9 Dual Feasibility Recovery ODP (Dual-FR-ODP)

Maximize:

$$\begin{aligned}
 (3.13a) \quad & - \sum_{j,t} \lambda_{j,t} \left((v_{j,t}^k - l_{j,t}^k)^2 + (2P_{j,t}^k)^2 + (2Q_{j,t}^k)^2 \right. \\
 & \left. - 2(v_{j,t}^k - l_{j,t}^k)v_{j,t}^k + 2(v_{j,t}^k - l_{j,t}^k)l_{j,t}^k - 8(P_{j,t}^k)^2 - 8(Q_{j,t}^k)^2 \right) + \gamma_{j5,t} - \gamma_{j6,t}
 \end{aligned} \tag{3.15a}$$

Subject to:

(3.13e) to (3.13g), (3.13i), (3.13k) to (3.13w)

$$(P_{j,t}) : \pi_{a,j,t} - \pi_{a,A_j,t} - 2\gamma_{j3,t} + \sum_g (\varpi_{2,j,t,g}^- - \varpi_{2,j,t,g}^+) - 8P_{j,t}^k \lambda_{j,t}^k = 0, \tag{3.15b}$$

$$\forall j \in \mathcal{N}_+, \forall t \in \mathcal{T}$$

$$(Q_{j,t}) : \pi_{r,j,t} - \pi_{r,A_j,t} - 2\gamma_{j4,t} + \sum_g (\rho_{2,j,t,g}^- - \rho_{2,j,t,g}^+) - 8Q_{j,t}^k \lambda_{j,t}^k = 0, \tag{3.15c}$$

$$\forall j \in \mathcal{N}_+, \forall t \in \mathcal{T}$$

$$\tag{3.15d}$$

$$(v_{i,t}) : -\pi_{v,i,t} + \sum_{j \in \mathcal{C}_i} \pi_{v,j,t} - \gamma_{i1,t} - \gamma_{i2,t} + \sigma_{i,t}^+ - \sigma_{i,t}^- - 2\gamma_{i7,t} - 2(v_{i,t}^k - l_{i,t}^k) \lambda_{i,t}^k = 0, \tag{3.15e}$$

$$\forall i \in \mathcal{N}_+, \forall t \in \mathcal{T}$$

$$(l_{i,t}) : \sum_g (l_{2,i,t,g}^- - l_{2,i,t,g}^+) - \gamma_{i1,t} + \gamma_{i2,t} + \eta_{i,t}^+ - \eta_{i,t}^- - 2\gamma_{i7,t} + 2(v_{i,t}^k - l_{i,t}^k) \lambda_{i,t}^k = 0, \tag{3.15f}$$

$$\forall i \in \mathcal{N}_+, \forall t \in \mathcal{T}$$

$$(f_{j,t}) : \lambda_{j,t} - \gamma_{j5,t} - \gamma_{j6,t} = 0, \quad \forall j \in \mathcal{N}_+, \forall t \in \mathcal{T} \tag{3.15g}$$

$$(s_{j,t}) : -v_{j,t} - \lambda_{j,t} = -\rho, \quad \forall j \in \mathcal{N}_+, \forall t \in \mathcal{T} \tag{3.15h}$$

$$\begin{pmatrix} \gamma_{i5,t} \\ \gamma_{i6,t} \\ \gamma_{i7,t} \end{pmatrix} \in \mathbb{L}^3, \quad \forall i \in \mathcal{N}_+, \forall t \in \mathcal{T} \tag{3.15i}$$

Results

This chapter is dedicated to numerical experiments that will be performed on a real dataset. The goal of this chapter is to validate the methodology presented in the previous chapters and understand to what extent line reinforcement, fuse limits and storage investment are capable of addressing the challenges of the DSO in the context of high penetration of DERs.

4.1 Description of the dataset

We use data from a real distribution network with real generation and load profiles. Our dataset is a slightly simplified version of the data used in Niels Leemput PhD thesis [11] which is a real urban feeder topology that was provided for the EIT-KIC InnoEnergy EVCity project [12]. This simplified version was used in Arnaud Fabri's master thesis [13].

4.1.1 Distribution grid

We will use two different distribution grids. The first one is a 29 households distribution network made of one main feeder (primary line) and secondary lines connecting the households to the primary line (see Figure 4.1). Both types of lines have the same characteristics. There are therefore 29 households nodes, 29 connection nodes and the substation node which connects the LV network to a medium voltage network through a transformer of maximum power rating of 250kV, for a total of 59 nodes. All households are assumed to be connected to the same phase, with a rated neutral-to-phase voltage of 230V. In what concerns the distances, the distance between the substation node and the first connection node is 350m. Then, the distance between two successive connection nodes is 7.2m until node 17 where there is a gap of 30m until the next connection node. After that, the nodes are 8.3m apart. Each house is located at a distance of 10m to its corresponding connection node. The characteristics of the lines are summarized in table 4.1.

Impedance	$0.31 + i0.0713$	$[\Omega \text{ km}^{-1}]$
Current limit	210	[A]

Table 4.1: Characteristics of the line.

The second system we use is exactly the same grid but for which we keep only the 10 first nodes.

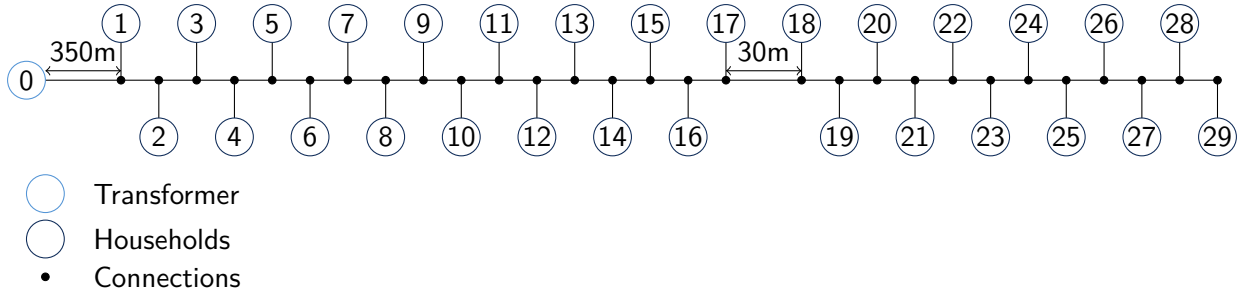


Figure 4.1: The real distribution network used.

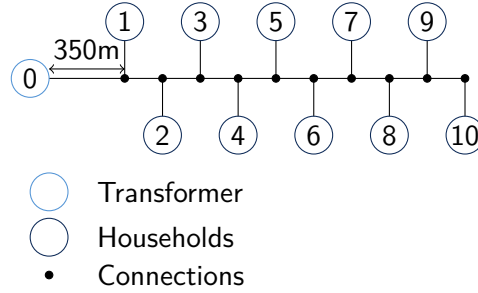


Figure 4.2: The reduced distribution network.

The reason we will also use this dataset is because the computations can become slow when the number of nodes is too high, which makes it challenging if we want to solve the problem with different values of the parameters. Therefore, for certain experiments, we will run them on the smaller set. It is schematically represented in figure 4.2.

4.1.2 Residential load and generation

We use real single-phase household electric power consumption profiles that were sampled in 2008, with a 1 hour time resolution. We also have real PV power generation profiles for all these households that are based upon measurements at an installation of the KU Leuven, also with a 1 hour resolution. The horizon used is one week and the profiles were acquired in May.

4.1.3 Battery storage modeling

For the parameters of the battery storage modeling, we use the same assumptions and data as [13]. Therefore, we suppose negligible dissipation rate in the battery, we set the minimum input and output rate to 0 and we use the same data derived from the Tesla PowerWall 2, which gives us the parameters summarized in table 4.2.

Investment cost (C_s)	4.435	[€/MW h/h]
Maximum input rate ($\overline{p_i^{in}}$)	$0.37 f_i$	[MW h ⁻¹]
Maximum output rate ($\overline{p_i^{out}}$)	$0.37 f_i$	[MW h ⁻¹]
Charging factor (ξ_{in})	0.975	
Discharging factor (ξ_{out})	0.975	

Table 4.2: Parameters of the storage modeling.

where f_i is the total storage capacity invested in node i .

4.1.4 Voltage control

The European standard for voltage control allows a deviation of +10%/-10% from the nominal value (here 230V). However, these values should hold for the entire network and only a fraction of these deviations is accepted for each voltage level. In Flanders, the acceptable deviations for the LV network are +1.5%/-6% [11]. In this work, we fix the value of the voltage at the substation node and use the percentage deviations to derive the upper and lower bound for the square voltage magnitude. Values are given in table 4.3.

Voltage magnitude at root	0.23	[kV]
Squared voltage magnitude at root ($v_{0,t}$)	0.0529	[kV ²]
Maximum of the squared voltage magnitude (\bar{v})	0.0545	[kV ²]
Minimum of the squared voltage magnitude (\underline{v})	0.4674	[kV ²]

Table 4.3: Parameters of the voltage control.

4.1.5 Line reinforcement

In our experiments, we considered two possible choices of line. We have therefore $N_{\text{choices}} = 2$ and $\mathcal{G} = \{1, 2\}$. The first possibility is to keep the installed line with characteristics given in table 4.1 at a cost of $C_1 = 0$. The second possibility is to reinforce the network at a nonzero cost C_2 . To find a realistic cost for the line replacement, we rely on data used in Benoît Martin's PhD thesis [14]. The costs are summarized in Table 4.4.

Annualized building cost of line	2770	[€/km/year]
Total cost for one week	53.26	[€/km]

Table 4.4: Cost of line reinforcement.

The new lines have characteristics given in table 4.5.

Impedance	$0.26 + \mathbf{i}0.07$	[$\Omega \text{ km}^{-1}$]
Current limit	210	[A]

Table 4.5: Characteristics of the line.

4.1.6 Other parameters

Unless stated otherwise, the value for the other parameters that we use are given in table 4.6.

VOLL	8300	[€/MW h]
Cost of PV curtailment (C_+)	500	[€/MW h]
Cost of losses (C_l)	300	[€/MW h]
Maximum deviation from nominal value (δ)	0.1	
Budget parameter for load (Δ_{load})	10	
EV battery capacity (C)	24	[kW h]
Budget parameter for PV (Δ_2^{PV})	Δ_1^{PV}	
Initial penalty parameter (ρ^1)	0.01	
Growing rate of penalty parameter (τ)	2	
Maximum penalty parameter (ρ^M)	10^{12}	

Table 4.6: Parameters of the voltage control.

4.2 Impact of Δ_1^{PV}

In this section, we focus on the number of PV installations and evaluate its impact on DSO investment and operations. In particular, we wish to determine the number of PV installations above which it becomes favorable to invest in storage.

As the procedure to determine the parameter C_f that corresponds to a specific value of $x_{\text{unplanned}}^{\%}$ is cumbersome, we will use a fixed value of C_f to perform this analysis. Moreover, it makes the results more comparable.

Let us first show the behavior of the curtailment for different values of Δ_1^{PV} . We represent the unplanned curtailment with and without fuse limits as well as the total unplanned curtailment that takes place in the system (Figure 4.3).

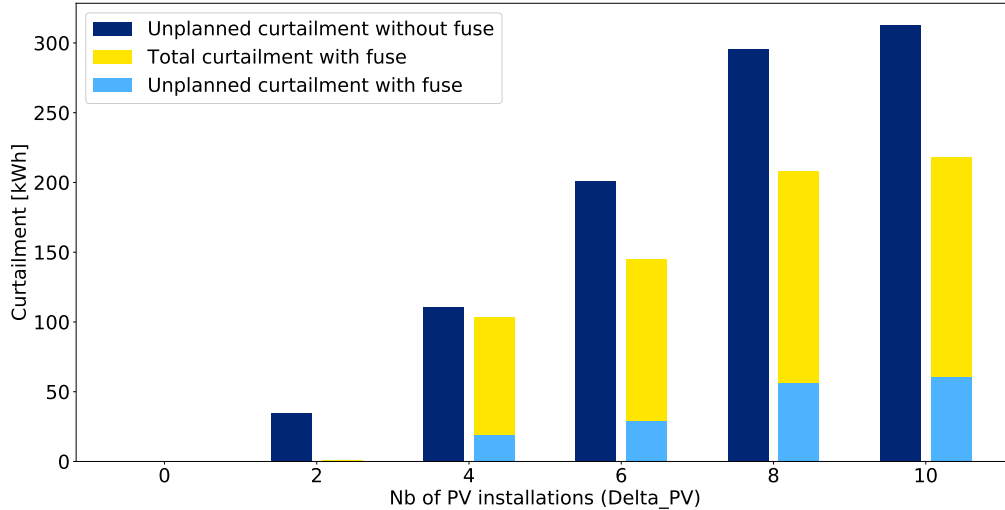


Figure 4.3: Total unplanned curtailment in the system for different number of PV installations.

Figure 4.3 shows that if we do not set any fuse limits, unplanned curtailment is needed to control voltage and current as soon as there are two PV installations in the system. Moreover, we can see that this unplanned curtailment without fuse limits (i.e. when $C_f = 0$), in dark blue in the bar chart, increases with Δ_1^{PV} . This proves that solar production is in this case a problem for the reliability of the network. In light blue, we can see the unplanned curtailment that remains when we add the fuse

limits. The value of C_f was chosen so that this unplanned curtailment is around 10% for $\Delta_1^{PV} = 10$. The total curtailment, which includes the planned curtailment, is shown in yellow.

Let's see now if storage investment is part of the optimal solution. The following figure represents the total optimal storage capacity in function of Δ_1^{PV} together with the maximum demand in light blue and the maximum reinjection in the network due to PV overproduction in yellow (Figure 4.4).

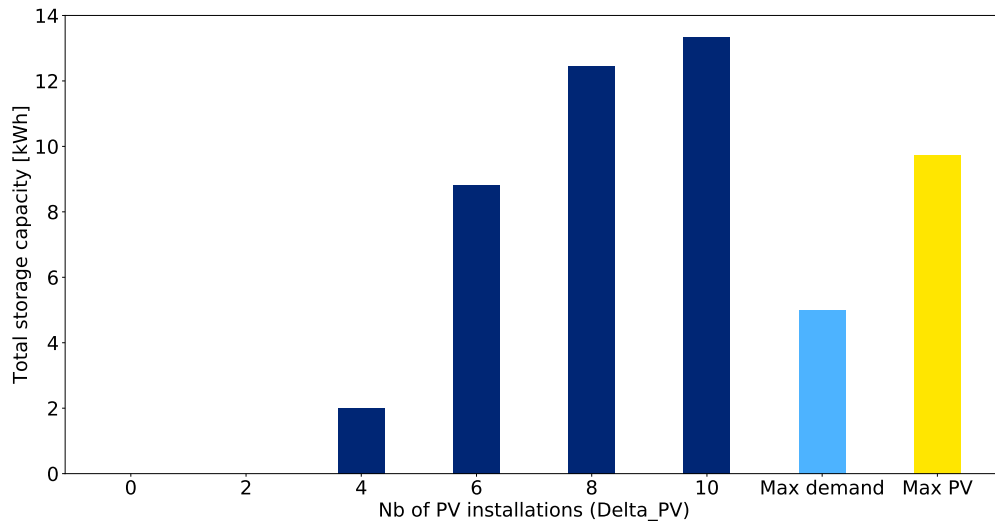


Figure 4.4: Total storage capacity invested in the system for different numbers of PV installations. In light blue, we show the sum of the demand in the whole network corresponding to the time step with maximum demand. In yellow, the maximum PV production after curtailment for $\Delta_1^{PV} = 10$.

We observe that it is favorable to invest in storage as soon as 4 houses have PV installations. Moreover, the installed capacity increases with the number of PV installations. This is of course very natural as there will be more solar production to be stored.

In the following figure, we show the distribution of the total investment and operational costs with respect to the different types of cost, in function of Δ_1^{PV} (Figure 4.5).

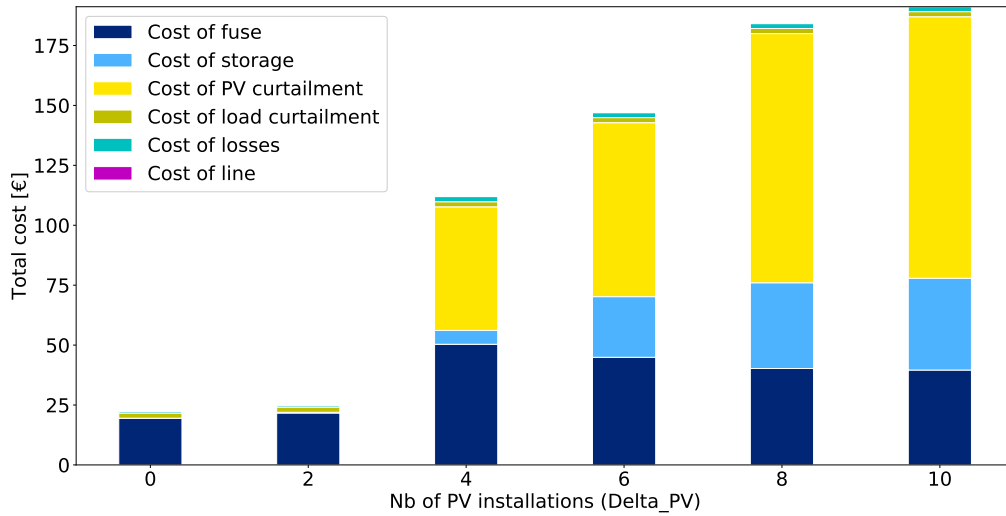


Figure 4.5: Distribution of the total cost for different numbers of PV installations.

On this figure, we first notice that the total cost increases with Δ_1^{PV} . This highlights the cost that congestion due to large solar production represents for the network operator. The cost of the line is zero in each case because it is not favorable to invest in a new line. We also observe that when $\Delta_1^{PV} = 2$, no PV curtailment takes place. This is because the small PV production in the network does not cause any congestion problem and the fuse limit can thus safely be placed at the maximum demanded injection. This can also be seen in figure 4.6 which represents the evolution of the fuse limits.

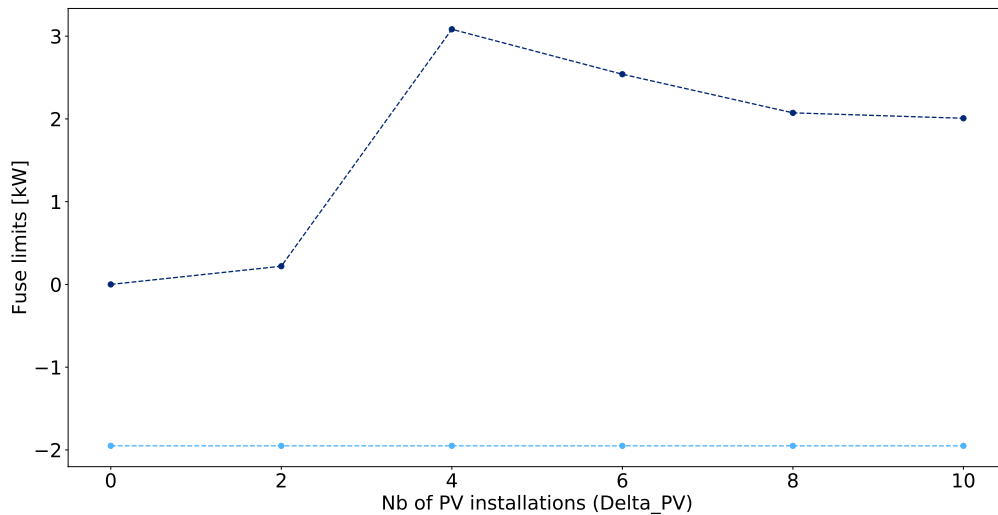


Figure 4.6: Fuse limits for different numbers of PV installations.

In what concerns the lower limit, the optimal value is the same for each value of Δ_1^{PV} and is slightly above the minimum value of the demanded injection (which is negative when the power is consumed). If we look more precisely at the curtailment profiles (Figure 4.7), we can see that the demand is curtailed for one hour at one particular house (house 4). So it is really the peak consumption that

is cut. The upper limit depends on Δ_1^{PV} . In our case, it increases until 4 and then decreases. The reason for this decrease is to be found in figure 4.3. Indeed, as Δ_1^{PV} increases, congestion in the network also increases and unplanned curtailment has to take place. This is curtailment that, even if we increase the upper fuse limit, would have had to occur. Therefore, it becomes better to decrease the fuse limit to save some fuse cost. We can also explain this by reasoning in terms of cost: there is a cost associated to higher fuse limit. The reason why it might be favorable to have a high limit, like when $\Delta_1^{PV} = 4$, is because it decreases the planned curtailment that is also costly. However, when $\Delta_1^{PV} = 6$ or more, the PV production is large and it tends to lead to congestion issues. Therefore, even if we have a high limit, we would have to curtail (in the form of unplanned curtailment). So the advantage of a high limit like for $\Delta_1^{PV} = 4$ disappears and it's better to decrease the limit.

To have more insight about how and where curtailment occurs, we show on figure 4.7 three typical injection profiles. In dark blue, we show the power that is actually injected in the network. The planned curtailment is shown in yellow while the unplanned curtailment is shown in cyan. Similarly, in light blue, we show the power that is withdrawn from the network, with the planned curtailed demand shown in magenta. Note that we do not observe any unplanned load curtailment.

The first profile corresponds to that of house 2 and is the typical profile of a house with a small PV installation. For this house, nothing is curtailed. The second profile is representative of a house with a large PV installation for which the production is highly curtailed but the peak demand of more than 2kW is also slightly curtailed. It is actually the only time and place for which the demand is not matched. The third profile is that of a house with a medium size installation, no planned curtailment occurs but there is a bit of unplanned curtailment.

In the next section, we analyze the impact of Δ^{EV} on the behavior of the system.

4.3 Impact of Δ^{EV}

We will now analyze the impact of the number of Electrical Vehicles on the behavior of the planning system. For this analysis, we fix Δ_1^{PV} to 10 and we make Δ^{EV} vary between 0 and 10.

Let us first show what the curtailment without and with fuse limits becomes on figure 4.8.

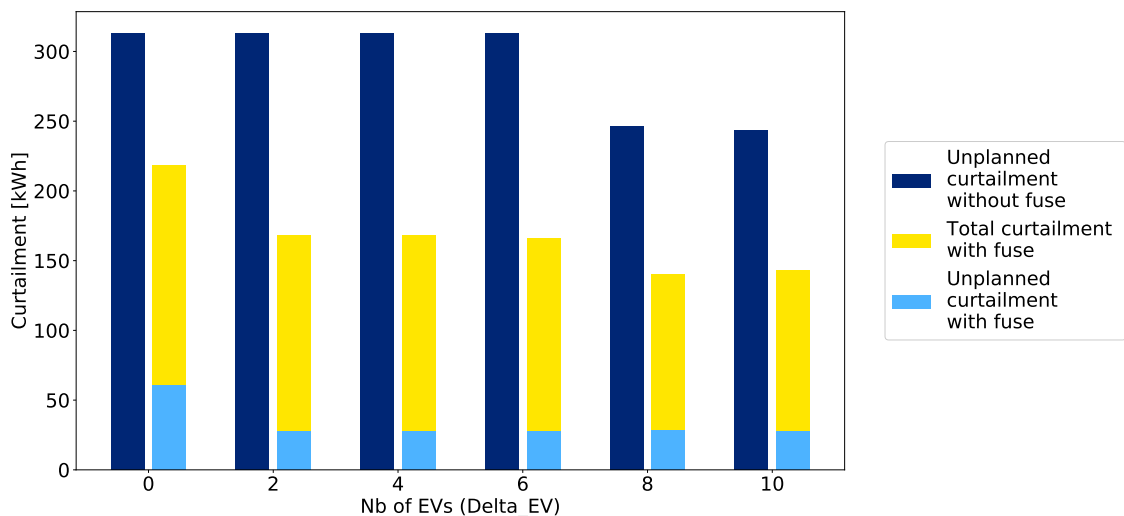


Figure 4.8: Total unplanned curtailment in the system for different number of PV installations.

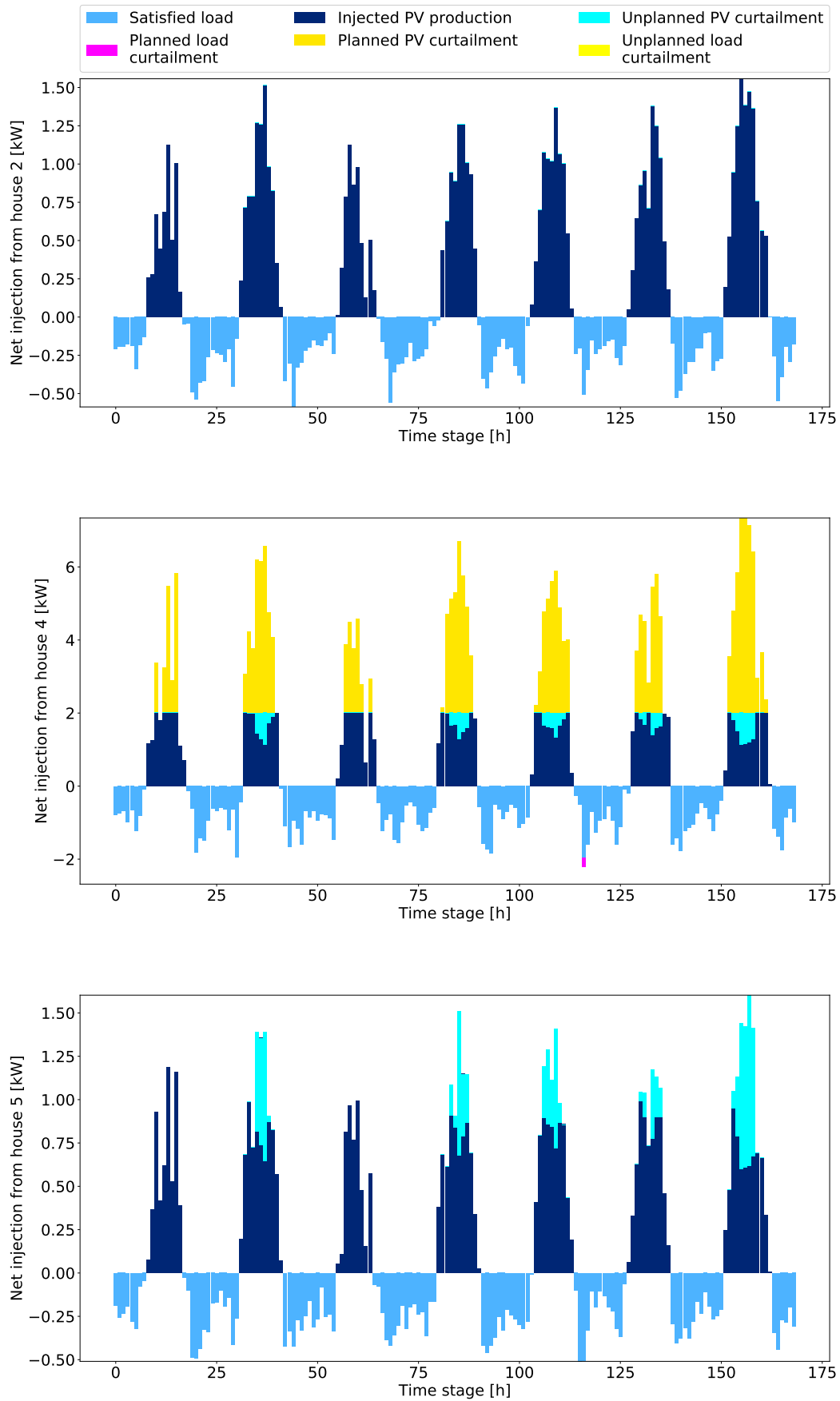


Figure 4.7: Typical curtailment profiles for representative houses.

We first notice that the total unplanned curtailment without fuse limits, in dark blue in the graph, is almost constant but drops when Δ^{EV} goes from 6 to 8. The fact that curtailment tends to decrease when we add EVs is because it enables to match better the demand with the overproduction. However, in our case, the decrease is limited. This can be understood by recalling that we work with a robust model that will always look for the worst case. The specific reason why there is a decrease between node 6 and 8 is because there is a line reinforcement when $\Delta^{EV} = 8$, as we will discuss later. Similarly, we show the profiles for $\Delta^{EV} = 10$ at house 2, 4 and 5 on figure 4.9

With this figure, we have a first preview of what it brings to have a robust solution : our algorithm finds that in the worst case, the EVs are charged during the night when there are no PV production. With a nonrobust solution, we would probably have found a solution that would have required much less curtailment.

The costs are shown in figure 4.10.

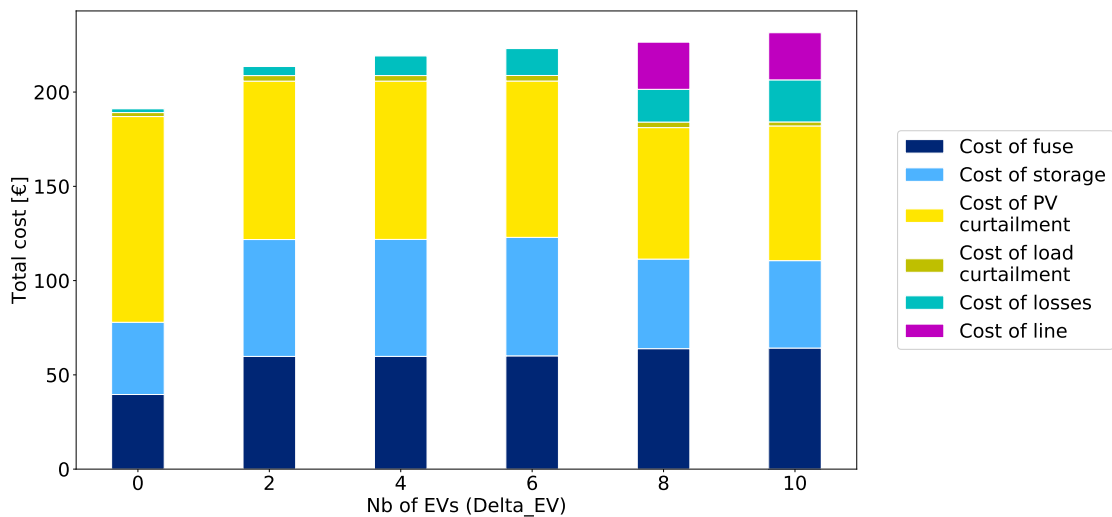


Figure 4.10: Repartition of the total cost for different numbers of EV installations.

The main difference with the costs obtained for the case without EVs and displayed in figure 4.5 is the cost of losses, which is now increased. Due to this increase in losses, it now becomes favorable to invest in a new line when there are 8 EVs or more. The new line enables to reduce the cost of losses as well as the cost of storage and of curtailment, as we can see on the figure.

The evolution of the fuse limits is quite different from the case without EVs. It is displayed in figure 4.11.

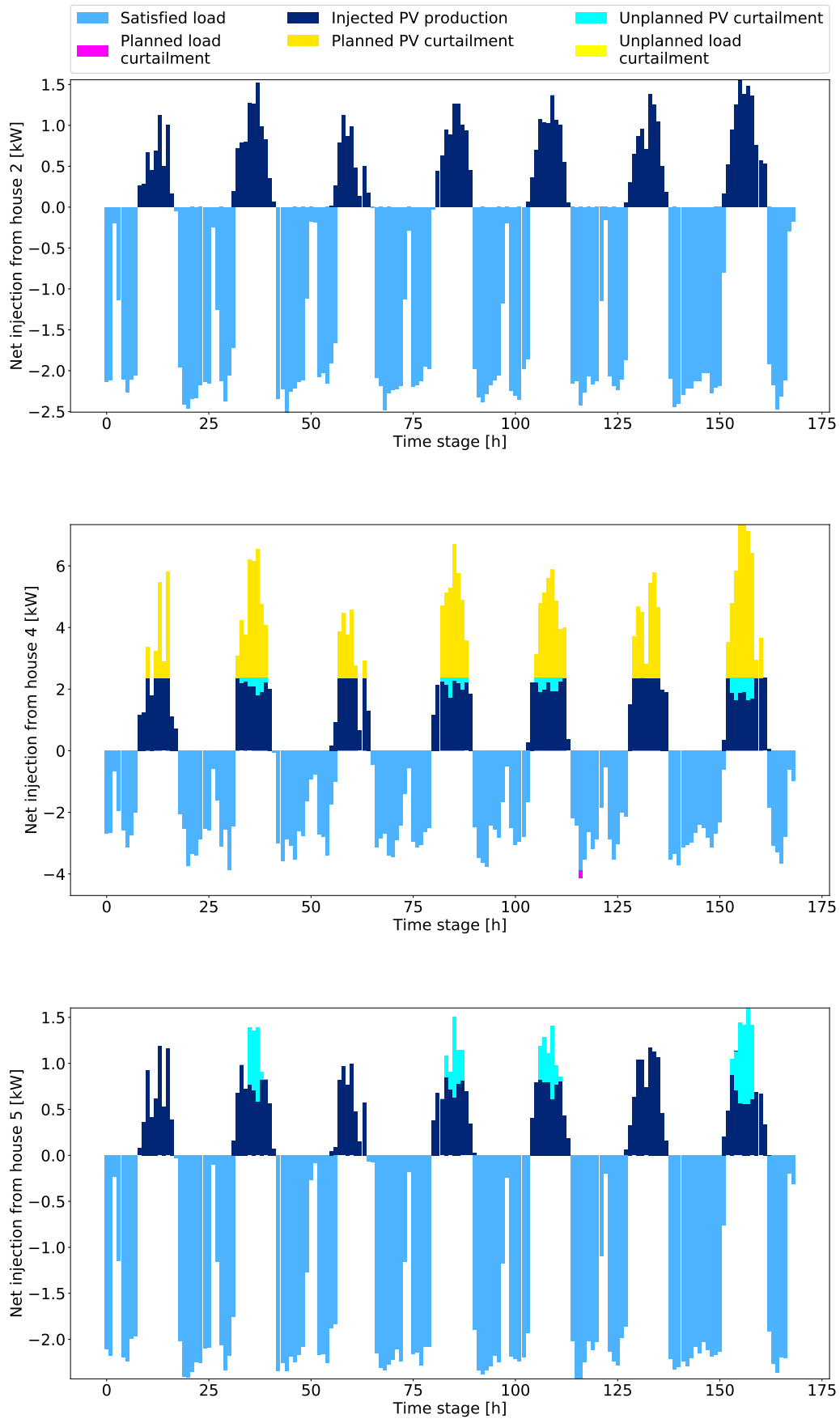


Figure 4.9: Typical curtailment profiles for representative houses with EV at every house.

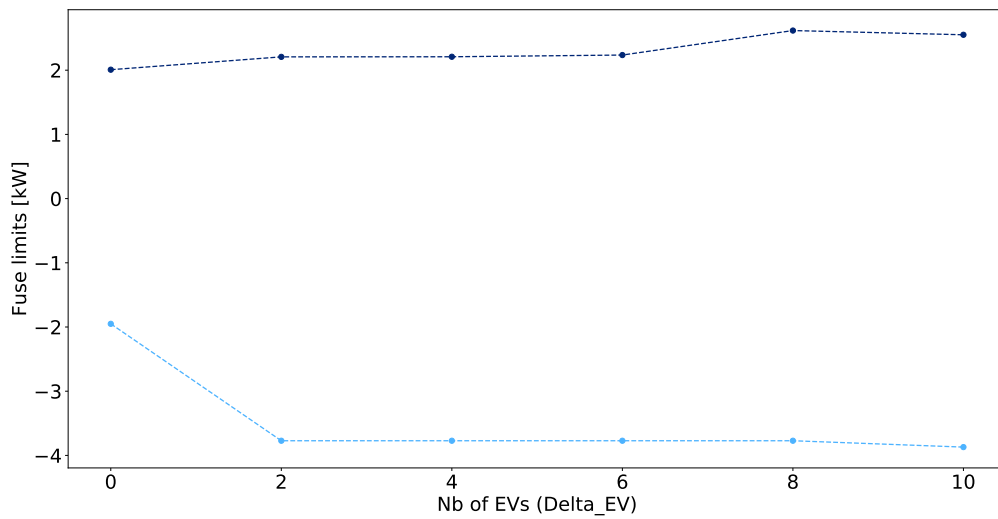


Figure 4.11: Fuse limits for different numbers of EVs.

The upper limits are very similar with the Δ^{EV} although it increases suddenly when the network is reinforced. The reason for this increase is because bigger lines can handle more reinjection without the need to resort to curtailment. The lower limit is obviously the same as the one of figure 4.6 when $\Delta^{EV} = 0$. When Δ^{EV} increases, the lower fuse limit goes down so that only the peak demand is curtailed. This peak demand is shown in figure 4.9 in the last profile where the curtailed demand is shown in magenta. This result is very similar to the one obtained for the case without EV where only the peak demand was slightly curtailed.

4.4 Evolution of DERs

By combining the two previous sections, we will now show the impact of an increasing share of DER, i.e. we will make both the number of PV installations and the number of EVs vary together. The histogram of the evolution of the cost in this case is shown in figure 4.12.

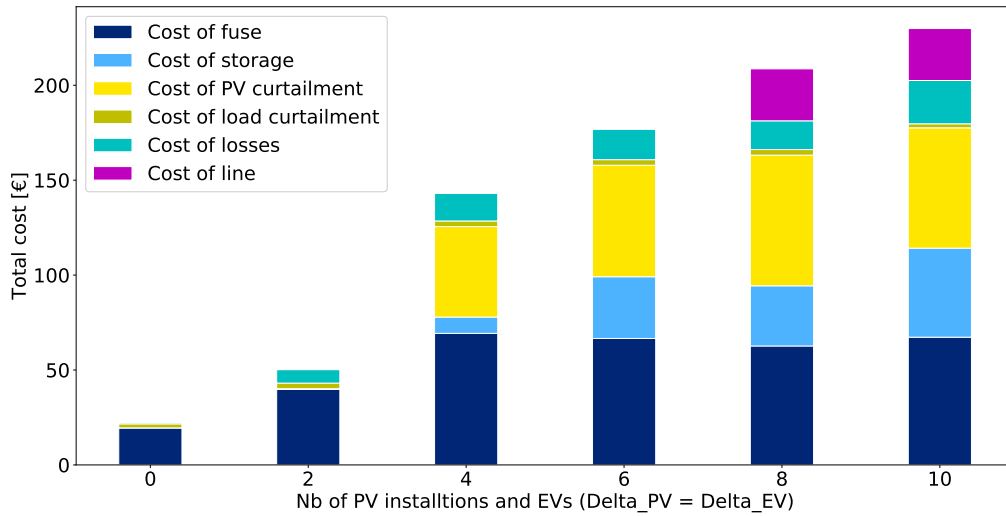


Figure 4.12: Evolution of the cost of the robust ODP with an increasing share of DER (PV installations and EVs). Note that we set $\Delta_1^{PV} = \Delta^{EV}$.

We observe that the solution is a mix of the two previous experiments : investment in storage is made as soon as there are 4 PV installations and 4 EVs and a new line is build when there are eight of them.

For this same experiment, the evolution of the curtailment and the fuse limits, similarly to the previous cases, are given respectively in figure 4.13 and 4.14.

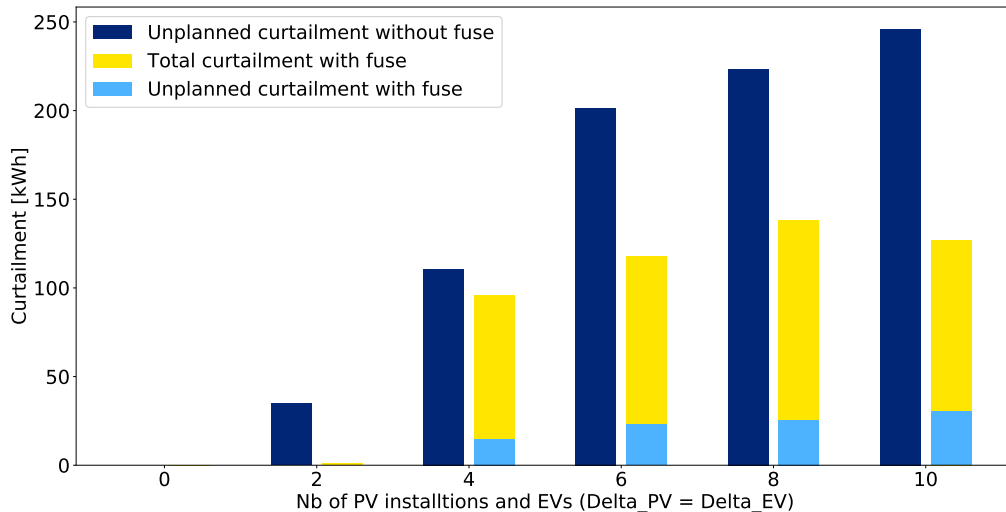


Figure 4.13: Total unplanned curtailment in the system for different number of DERs.

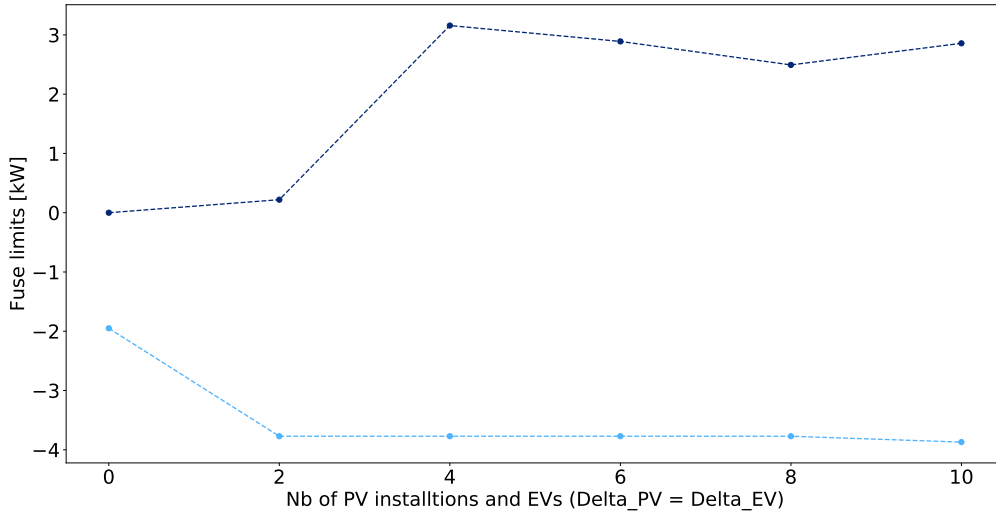


Figure 4.14: Fuse limits for different numbers of DERs.

Interestingly, the combination of a large number of PV installations and EVs yields a different patterns in the evolution of fuse limits than when only the number of PV installations was increasing and that was shown in Figure 4.6. Whereas then, the fuse limits kept decreasing with Δ_1^{PV} , here, the fuse limits increase from 8 to 10 PV installations and EVs. A larger investment in storage becomes favorable, which allows to curtail less PV production and to satisfy more demand.

4.5 Analysis of robustness

One of the main feature of our model is that it is robust to load and production uncertainties as well as to location and charging time of the EVs. In this section, we propose to analyze in more details the worst case behavior of the system with respect to these uncertainties.

4.5.1 Robustness on PV location

The first experiment that we will do is to compare our solution with the solution that we would have obtained if we had only imposed a total PV capacity in the whole network, distributed in each house. This is equivalent to fixing the value of u_i^{PV} to $\frac{\Delta_1^{\text{PV}}}{n}$, where n is the number of houses. This means that instead of having Δ_1^{PV} houses which have one full PV installation, all houses have a fraction of a full installation.

Let us fix Δ_1^{PV} to 6. The following figure compares the total cost in the case of the robust solution and in the case of fractional PV installations (Figure 4.15).

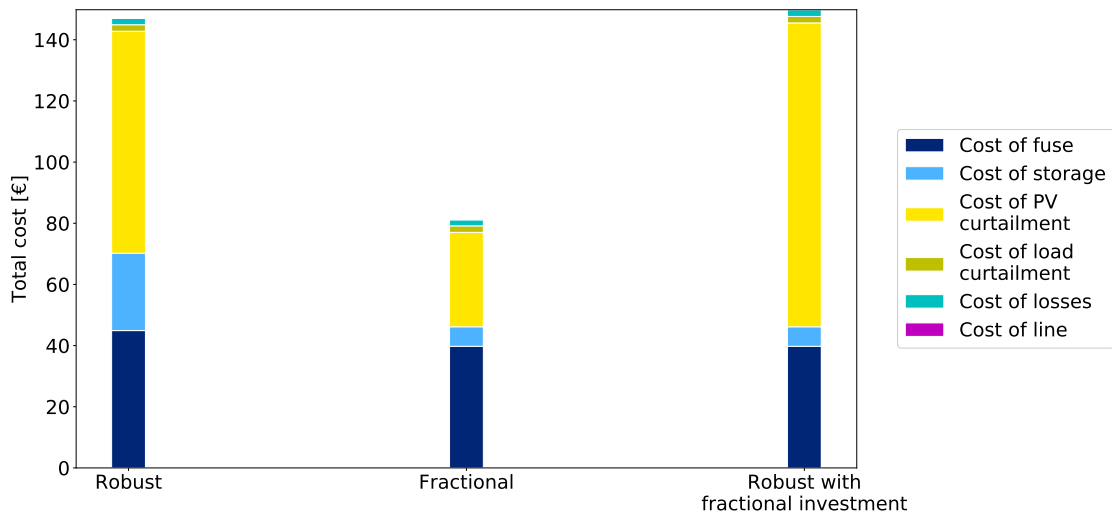


Figure 4.15: Comparison between the price in the case of the model robust and nonrobust to PV location. The case named *fractional* corresponds to Δ_1^{PV} being fixed to $\frac{6}{10}$ for each house whereas the case called *robust with fractional investment* means that Δ_1^{PV} is unfixed but we fix the investment decisions to those found by the fractional solution.

The total cost of the robust solution is almost twice the cost of the nonrobust one. This shows the importance for the DSO to have a solution that is robust to the location of PV installations. More particularly, we can see that the robust solution involves more curtailment of high PV production and invests more in storage. If we use the investment decisions of the fractional case with the worst-case profiles, we can see that the cost is higher than when we use the robust investment. This highlights, again, the advantage of having a robust solution.

4.5.2 Location in the worst case

It would also be interesting to see in which nodes the PV installations are located with our robust solution. To analyze that, we go back to the 29 households dataset. When we fix Δ_1^{PV} to 15 and Δ^{EV} to 0, we obtain the distribution of PV installations shown in figure 4.16.

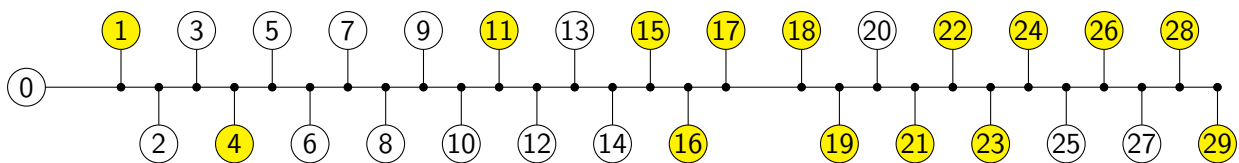


Figure 4.16: In yellow, the location of the PV installations in the network.

On this figure, we see that the PV systems tend to be located at the end of the line. The exceptions are due to the fact that the PV installations are all of different size. The algorithm will thus notice that it is worse to have a large installation at the beginning of the line compared to a small one at the end. If we artificially let all PV profiles be the same (equal to the average profile), the figure becomes :

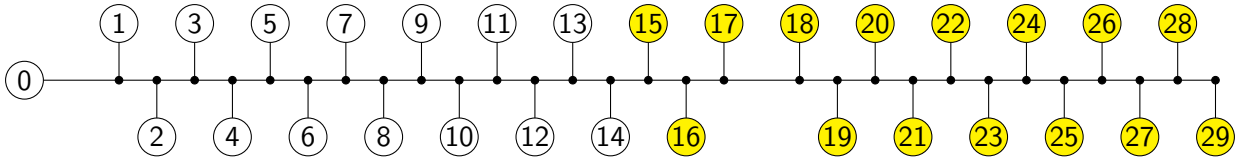


Figure 4.17: In yellow, the location of the PV installations in the network in the case of same production profiles for each house.

The reason for this pattern, as explained in [13], is that it is cheaper to reinject production that is closer to the substation node because the line losses will be reduced.

4.6 Gap of the Feasibility Recovery Procedure

Recall that at this stage, the solution that we obtained with algorithm 1 has no optimality guarantee. Indeed, we used the FRP and the solution of the SOCP relaxation to obtain a solution that is feasible and close to the solution of the relaxation. As a feasible solution, the corresponding value of the objective gives us an upper bound on the optimal solution. The optimal value of the relaxed problem is a lower bound. To give some insight on the value of the gap between the two bounds, we show them on figure 4.18 for the case where we make Δ_1^{PV} vary.

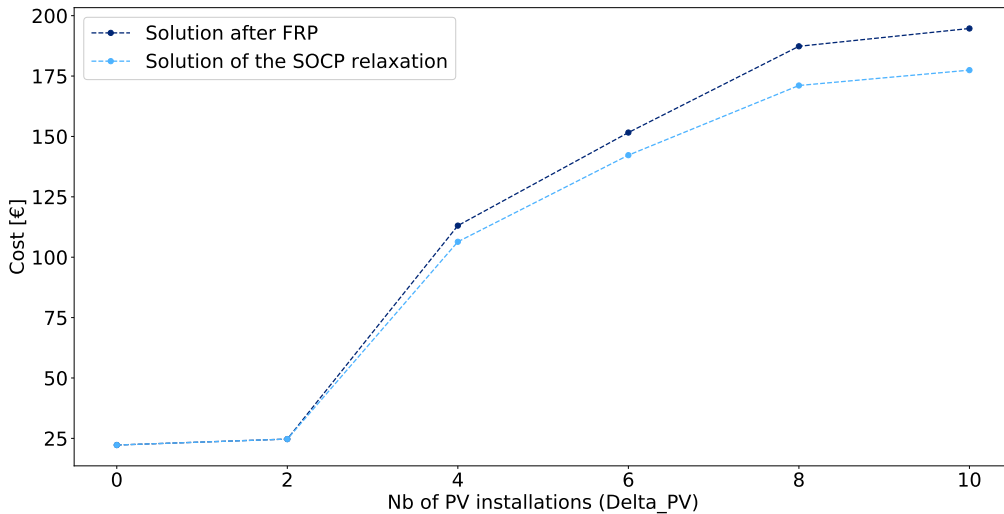


Figure 4.18: Evolution of the upper and lower bound of the solution when Δ_1^{PV} increases.

Note that, as part of the robust algorithm, the FRP has to be solved several times. We show here only the values of the gap for the last problem solved. We observe in figure 4.18 that the gap increases with Δ_1^{PV} . This is because the inexactness of the SOCP relaxation increases, too. Indeed, this inexactness increases when the curtailment of the PV production increases. As we can see on the graph, when no PV curtailment takes place (i.e. for $\Delta_1^{\text{PV}} = 0$ and 2), the gap is zero. The close link between the PV curtailment and the inexactness of the SOCP relaxation can be explained because it breaks assumption (A_2). This assumption can be understood as follows : the SOCP relaxation allows to recover the feasibility of the convex solution by throwing away electricity at each node, i.e. to curtail without any cost. This curtailment is thus curtailment that does not necessarily have to take place for physical reasons. This is incompatible with the modeling of fuse limits, that should be

chosen with respect to the real physical curtailment. Therefore, in our model, this curtailment has a cost, which explains why whenever PV curtailment should happen for physical reasons, the SOCP relaxation is inexact and we need to go through the FRP.

Finally, note also that it is not because there is a nonzero gap in figure 4.18 that the solution we found is not optimal. In fact, in the initial paper which proposes the FRP ([5]), the authors argue that if the parameters of the algorithm are chosen delicately, the solution found by FRP will be very close, if not equal, to the optimal solution.

4.7 Execution time and number of iterations

In this section, we discuss the performances of the algorithm. First, we show the time taken by each model of the complete algorithm for a fixed choice of line in Figure 4.19. There are six different models to solve. First, there are three models solved during the SOCP relaxation: the first-stage problem where investment decisions are made, the second stage with a fixed $d_{i,t}$ parameter and the second stage with fixed $\zeta_{i,t}$. Note that the first-stage and the second stage with fixed d are both SOCP whereas the second stage with fixed ζ is a Linear Program (LP), in view of our uncertainty set presented in section 2.6. All experiments were carried out on a laptop with Intel i7-5500U CPU and 8 GB memory. The optimization models were coded in GAMS and both the quadratic and linear problems were solved with Gurobi.

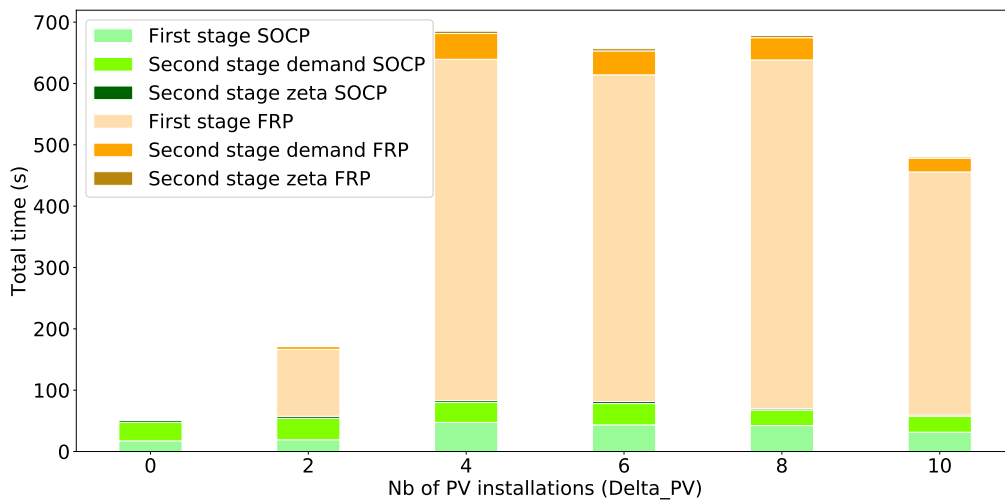


Figure 4.19: Total running time of the algorithm for each type of model. The time is expressed in seconds of wall-clock time.

On this figure, we first observe that the time increases a lot from 0 to 4 PV installations. This increase is clearly due to the fact that the SOCP relaxation is exact at each iteration when there are 0 PV installation whereas for 4 PV installations, it is inexact and we have to go through the costly FRP. The case of 2 PV installations is a bit in-between : there is a small infeasibility for the case $C_f = 0$ but no infeasibility for the nonzero value of C_f . Then, the time is more or less constant until 10 PV installations where there is a small drop. This drop is partly due to the fact that there is no more uncertainty on the PV location as all houses have an installation.

In the table below (Table 4.7) we show the maximum number of iterations before convergence for each part of our algorithm. The parts of the algorithm that require convergence are the following :

1. The alternating direction method to solve the bi-conic problem.
2. The master-slave iterations to find the worst case of the uncertainty.
3. The number of iterations of the Feasibility Recovery Procedure.

Type of loop	$\Delta_1^{PV} = 0$	$\Delta_1^{PV} = 2$	$\Delta_1^{PV} = 4$	$\Delta_1^{PV} = 6$	$\Delta_1^{PV} = 8$	$\Delta_1^{PV} = 10$
Alternating directions	1	2	2	2	2	2
Worst case	2	2	3	3	2	2
Feasibility recovery	0	10	10	10	10	10

Table 4.7: Number of iterations for each type of loop.

This table shows that the alternating direction converges quickly to solve the bi-conic problem, i.e. in one or two iterations. It also shows that as expected, it is slightly more complicated to find the worst case with an intermediate value of Δ_1^{PV} . Finally, we observe that the FRP always converges in the same number of iterations (10). This corresponds to the iteration number at which ρ becomes of the same order of magnitude than the cost of the problem.

4.8 Conclusion to the real case analysis

In this chapter, we analyzed the behavior of our robust algorithm on a real distribution network. There are three main conclusions that we can draw from this real case study :

1. In the current state of the development of storage technologies, with realistic prices for line reinforcement and with realistic generation profiles, investing in batteries and installing new lines can help DSOs to reduce curtailment and their operational cost while reducing the discrimination of the customers along the line.
2. Having a solution that is robust to load and generation uncertainties brings to light the true value of storage in a distribution grid.
3. The combination of the willingness to have a robust solution and deciding on fuse limits increase greatly the complexity of the problem.

Conclusion

Context

As the electric power system is becoming more and more distributed and digitized, the Distribution System Operators face new challenges. To overcome these challenges, the role of the DSO should change completely. Whereas its role has always been to plan the investment in the network so that production could match the demand at any time, it will now have to include a real-time operation of the network to manage fuse limits and storage capacities. In one word, we could say that the DSO will have a much more active role in the operations of its network. To help in this transition, new decision-making tools will have to be developed.

For the time being, there are many issues in the way distribution systems with high share of DERs are managed. Indeed, DSOs tend to rely a lot on curtailment to maintain a high level of reliability of the electricity delivered to the customers. This is of course a problem for meeting the objectives on the share of electricity coming from renewable energy, but it is also a problem as it tends to discriminate people regarding their location in the network, which is often seen as problematic. The new tools should take these issues into account.

Besides the necessity for DSOs in developed countries to use new techniques to integrate renewable energies in the grid, these techniques are also important for developing countries, in which access to electricity can be a major issue for part of the population. As it is noted in [14], a majority of people who lack electricity live in rural areas. In that same work, it is argued that decentralized electrification is often a good option for providing these people with access to energy. In this context, the number of low-voltage micro-grids could rise in the coming years. The operations of these grids will also necessitate decision-making tools that can take into account distributed production and handle uncertainty in an appropriate way.

Summary

In this master thesis we proposed a new decision-making framework which aims at helping DSOs to couple the planning and the operations of their network in the context of large amount of DERs. We first presented a model for finding the optimal fuse limits, storage investment, line characteristics and power flow in the network. We then modeled the uncertainty on solar panels location, solar production, electrical vehicles location, charge timing and residential load. We showed how our problem can be solved in a robust way with respect to the uncertainty set defined. Finally, we validated our model

and the solution in experiments performed on a real distribution network with realistic production and load profiles and we discussed to what extent this new tool can help DSOs to overcome the challenges of the electric power system transition.

Through the real case application, we gave evidence in support of the argument stating that fuse limits are appropriate to reduce the curtailment in the network and to avoid important discrimination along the line. We showed that storage investment can reduce the investment and operational costs of the DSOs and we have quantified the share of DERs above which it becomes interesting to reinforce the network. We also characterized the advantages that a robust solution represents.

The main limitation of this work is the inefficiency of the robust algorithm that prevents the solution in its current state to be applied to large network. Although we showed that the solution time is reasonable for the 10 nodes and one week horizon real case, the problem appears intractable in its current form. This is because the SOCP solvers are not yet efficient enough to solve large problems such as ours. However, we can hope that in the future, their efficiency will improve and that our problem will become tractable. Moreover, it is possible that other algorithms than the standard barrier method are more efficient in this particular case.

Research perspectives

Probably one of the most important direction for further research would be to come up with techniques to speed up the algorithm and make the problem tractable. One idea that it would be worth exploring is the use of distributed optimization to leverage the increasing power of parallel computing. Moreover, it should be noted that our problem has intrinsically a distributed nature as some of the optimization variables involved are geographically localized in different places. In the future, we could imagine that a processor would be located at each node of the physical network and would communicate with a central processor that would process the investment variables and the information coming from every node. For the parallelization, algorithms like the Alternating Directions Method of Multipliers (ADMM) have proved to be well suited for conic problems [15]. A similar idea has already been proposed in [16] with the proximal message passing method, which is a version of ADMM. In their solution, each node in the network communicates with its neighbors and solve its own optimization problem to solve the global OPF. Generalization of this technique to our problem could be possible and would help to speed up the execution time.

In the same idea, parallel primal-dual interior-point method has recently been proposed in [17] to solve the DCOPF. The idea is to exploit the special structure of the OPF equations to solve the large sparse linear system involved in the primal-dual interior point method. It could be interesting to investigate the possibility to extend this technique to the conic problem of the SOCP relaxation of the ACOPF.

Besides the geographically decentralized nature, note also that the two-stage master-slave algorithm 3.2 could, with little changes, be parallelized as the different second-stage problems depend only on the first-stage decision but are mutually independent.

Bibliography

- [1] I. Pérez-Arriaga, C. Knittle, and M. E. Initiative, *Utility of the Future: An MIT Energy Initiative Response to an Industry in Transition*. MIT Energy Initiative, 2016.
- [2] M. Liebreich, "In search of the miraculous." *Bloomberg New Energy Finance Summit.*, 2016.
- [3] D. Bertsimas and M. Sim, "The price of robustness," vol. 52, pp. 35–53, 02 2004.
- [4] A. Lorca and X. Sun, "The adaptive robust multi-period alternating current optimal power flow problem," vol. PP, pp. 1–1, 08 2017.
- [5] W. Wei, J. Wang, N. Li, and S. Mei, "Optimal power flow of radial networks and its variations: A sequential convex optimization approach," *IEEE Transactions on Smart Grid*, vol. 8, no. 6, pp. 2974–2987, Nov 2017.
- [6] M. Farivar and S. H. Low, "Branch flow model: Relaxations and convexification 2014;part i," *IEEE Transactions on Power Systems*, vol. 28, no. 3, pp. 2554–2564, Aug 2013.
- [7] —, "Branch flow model: Relaxations and convexification 2014;part ii," *IEEE Transactions on Power Systems*, vol. 28, no. 3, pp. 2565–2572, Aug 2013.
- [8] C. ISO. (2017) Impacts of renewable energy on grid operations. [Online]. Available: <https://www.caiso.com/Documents/CurtailmentFastFacts.pdf>
- [9] A. L. Soyster, "Convex programming with set-inclusive constraints and applications to inexact linear programming," *Operations Research*, vol. 21, no. 5, pp. 1154–1157, 1973. [Online]. Available: <http://www.jstor.org/stable/168933>
- [10] A. Ben-Tal and A. Nemirovski, "Robust solutions of linear programming problems contaminated with uncertain data," *Mathematical Programming*, vol. 88, no. 3, pp. 411–424, Sep 2000. [Online]. Available: <https://doi.org/10.1007/PL00011380>
- [11] N. Leemput, "Grid-supportive charging infrastructure for plug-in electric vehicles," *PhD Thesis*, 2015.
- [12] A. Delnooz and C. Mol, "State-of-the-art in business models for charging services: the evcity approach," 11 2012.
- [13] A. Fabri, "Value of storage in smart grids," Master's thesis, Ecole polytechnique de Louvain, Université catholique de Louvain, 2017, prom. : Papavasiliou, Anthony ; de Maere d'Aertrycke, Gauthier.
- [14] B. Martin, "Autonomous microgrids for rural electrification: joint investment planning of power generation and distribution through convex optimization," Ph.D. dissertation, Ecole polytechnique de Louvain, Université Catholique de Louvain, 2018.

- [15] S. Boyd, N. Parikh, E. Chu, B. Peleato, and J. Eckstein, "Distributed optimization and statistical learning via the alternating direction method of multipliers," *Foundations and Trends® in Machine Learning*, vol. 3, no. 1, pp. 1–122, 2011. [Online]. Available: <http://dx.doi.org/10.1561/22000000016>
- [16] M. Kraning, E. Chu, J. Lavaei, and S. Boyd, "Dynamic network energy management via proximal message passing," *Found. Trends Optim.*, vol. 1, no. 2, pp. 73–126, Jan. 2014. [Online]. Available: <http://dx.doi.org/10.1561/24000000002>
- [17] A. Minot, Y. M. Lu, and N. Li, "A parallel primal-dual interior-point method for dc optimal power flow," in *2016 Power Systems Computation Conference (PSCC)*, June 2016, pp. 1–7.
- [18] A. Papavasiliou, "Analysis of distribution locational marginal prices," *IEEE Transactions on Smart Grid*, vol. PP, no. 99, pp. 1–1, 2017.

Chapter A

Evolution of the power price in a path graph

This section presents the detailed computations for deriving the formula of the evolution of the LMP. After that, the results are validated graphically and a physical interpretation of this evolution is given.

For each $i \in \{1, \dots, n-1\}$, let us combine the dual constraints to eliminate the variables γ_i . We have

$$\begin{cases} 2\gamma_{i1} = -\pi_{v,i} + \pi_{v,i+1} - (x_i^2 + r_i^2)\pi_{v,i} + r_i\pi_{a,i-1} + x_i\pi_{r,i-1} - r_i \\ 2\gamma_{i2} = -\pi_{v,i} + \pi_{v,i+1} + (x_i^2 - r_i^2)\pi_{v,i} - r_i\pi_{a,i-1} - x_i\pi_{r,i-1} + r_i \\ 2\gamma_{i3} = 2r_i\pi_{v,i} + \pi_{a,i} - \pi_{a,i-1} \\ 2\gamma_{i4} = 2x_i\pi_{v,i} + \pi_{r,i} - \pi_{r,i-1} \end{cases}$$

$$\begin{aligned} \Leftrightarrow & \left(-\pi_{v,i} + \pi_{v,i+1} - (x_i^2 + r_i^2)\pi_{v,i} + r_i\pi_{a,i-1} + x_i\pi_{r,i-1} - r_i \right)^2 \geq \\ & \left(-\pi_{v,i} + \pi_{v,i+1} + (x_i^2 - r_i^2)\pi_{v,i} - r_i\pi_{a,i-1} - x_i\pi_{r,i-1} + r_i \right)^2 \\ & + \left(2r_i\pi_{v,i} + \pi_{a,i} - \pi_{a,i-1} \right)^2 + \left(2x_i\pi_{v,i} + \pi_{r,i} - \pi_{r,i-1} \right)^2 \end{aligned}$$

$$\begin{aligned} \Leftrightarrow & -4r_i\pi_{v,i}\pi_{a,i-1} - 4x_i\pi_{v,i}\pi_{r,i-1} + 4(x_i^2 + r_i^2)\pi_{v,i}^2 - 4(x_i^2 + r_i^2)\pi_{v,i}\pi_{v,i+1} + 4r_i\pi_{v,i+1}\pi_{a,i-1} \\ & + 4x_i\pi_{v,i+1}\pi_{r,i-1} + 4r_i(\pi_{v,i} - \pi_{v,i+1}) \geq 4r_i^2\pi_{v,i}^2 + 4x_i^2\pi_{v,i}^2 + (\pi_{a,i} - \pi_{a,i-1})^2 + 4r_i\pi_{v,i}(\pi_{a,i} - \pi_{a,i-1}) \\ & + (\pi_{r,i} - \pi_{r,i-1})^2 + 4x_i\pi_{v,i}(\pi_{r,i} - \pi_{r,i-1}) \end{aligned}$$

$$\begin{aligned} \Leftrightarrow & 4r_i\pi_{v,i+1}\pi_{a,i-1} + 4x_i\pi_{v,i+1}\pi_{r,i-1} - 4(x_i^2 + r_i^2)\pi_{v,i}\pi_{v,i+1} \\ & - (\pi_{a,i} - \pi_{a,i-1})^2 - (\pi_{r,i} - \pi_{r,i-1})^2 + 4r_i(\pi_{v,i} - \pi_{v,i+1}) \geq 4r_i\pi_{v,i}\pi_{a,i} + 4x_i\pi_{v,i}\pi_{r,i} \end{aligned}$$

which can be written as

$$4r_i\pi_{v,i+1}\pi_{a,i-1} + 4x_i\pi_{v,i+1}\pi_{r,i-1} - C \geq 4r_i\pi_{v,i}\pi_{a,i} + 4x_i\pi_{v,i}\pi_{r,i}$$

with

$$C = 4(x_i^2 + r_i^2)\pi_{v,i}\pi_{v,i+1} + (\pi_{a,i} - \pi_{a,i-1})^2 + (\pi_{r,i} - \pi_{r,i-1})^2 - 4r_i(\pi_{v,i} - \pi_{v,i+1})$$

If we separate the active and the reactive power and we consider the case of an equality, we are left with

$$4r_i\pi_{v,i+1}\pi_{a,i-1} - 4r_i^2\pi_{v,i}\pi_{v,i+1} - (\pi_{a,i} - \pi_{a,i-1})^2 + 4r_i(\pi_{v,i} - \pi_{v,i+1}) = 4r_i\pi_{v,i}\pi_{a,i}$$

$$\Leftrightarrow 4r_i\pi_{v,i+1}\pi_{a,i-1} - 4r_i^2\pi_{v,i}\pi_{v,i+1} - \pi_{a,i}^2 + 2\pi_{a,i}\pi_{a,i-1} - \pi_{a,i-1}^2 + 4r_i(\pi_{v,i} - \pi_{v,i+1}) = 4r_i\pi_{v,i}\pi_{a,i}$$

$$\Leftrightarrow \pi_{a,i-1}^2 + (-2\pi_{a,i} - 4r_i\pi_{v,i+1})\pi_{a,i-1} + 4r_i^2\pi_{v,i}\pi_{v,i+1} + \pi_{a,i}^2 + 4r_i\pi_{v,i}\pi_{a,i} - 4r_i(\pi_{v,i} - \pi_{v,i+1}) = 0$$

$$\Leftrightarrow \pi_{a,i-1}^2 + F\pi_{a,i-1} + E = 0$$

with

$$\begin{cases} F^2 = 4\pi_{a,i}^2 + 16r_i^2\pi_{v,i+1}^2 + 16r_i\pi_{v,i+1}\pi_{a,i} \\ 4E = 4\pi_{a,i}^2 + 16r_i^2\pi_{v,i}\pi_{v,i+1} + 16r_i\pi_{v,i}\pi_{a,i} - 16r_i(\pi_{v,i} - \pi_{v,i+1}) \end{cases}$$

The solution is

$$\pi_{a,i-1} = \frac{-F \pm \sqrt{F^2 - 4E}}{2} = \pi_{a,i} + 2r_i\pi_{v,i+1} \pm 2\sqrt{r_i^2\pi_{v,i+1}(\pi_{v,i+1} - \pi_{v,i}) + r_i\pi_{a,i}(\pi_{v,i+1} - \pi_{v,i}) - r_i(\pi_{v,i+1} - \pi_{v,i})}$$

Power produced This is the case where the net injection is positive. It corresponds to the solution with a positive sign. The results are indeed similar in theory and in the model, as shown on figure A.1.

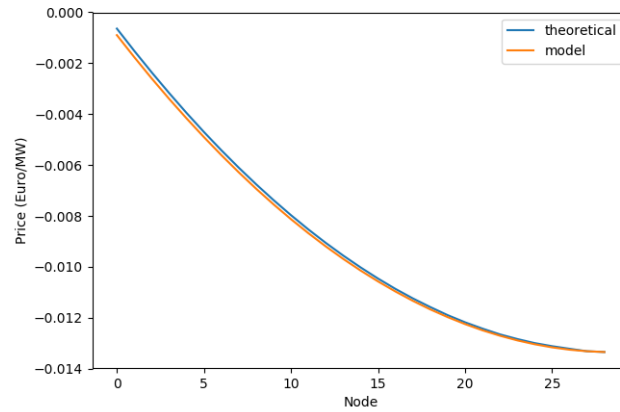


Figure A.1: Comparison between the evolution of the price along the line in theory and when the model is solved. This is the case of produced power at each node.

Based on [18], we can have a physical interpretation of this evolution of the price along the line. Indeed, this evolution is closely linked with the optimal value of voltage at each node. The evolution of voltage along the line is as follows (Figure A.2)

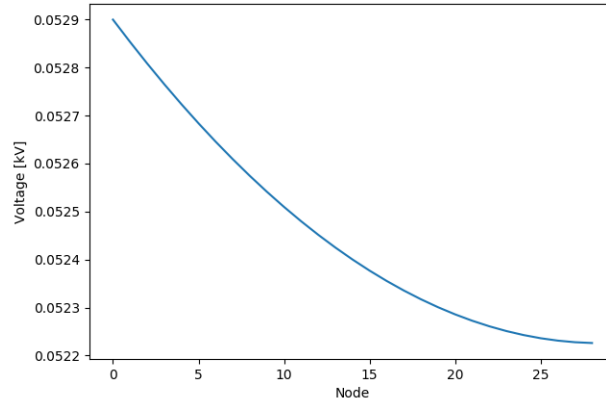


Figure A.2: Evolution of the optimal value of the voltage along the line.

We observe that the voltage at node $i + 1$ is lower than the voltage at node i . This means that by marginally increasing the injected power at node $i + 1$, we will make the voltage at that node decrease. Consequently, the current on the line will (see figure in [18]) increase and thus make the objective value increase so the price at node $i + 1$ will be positive and higher than the price at node i .

Power consumed In this case, prices are positive and it makes sense that the active power price increase along the line. The second solution (minus sign) should thus be chosen. In this case, again, theory predicts well the behavior of the prices as obtained when solving the model, provided we change Ohm's law constraints so that it yields increasing dual variables. The results are shown on figure A.3.

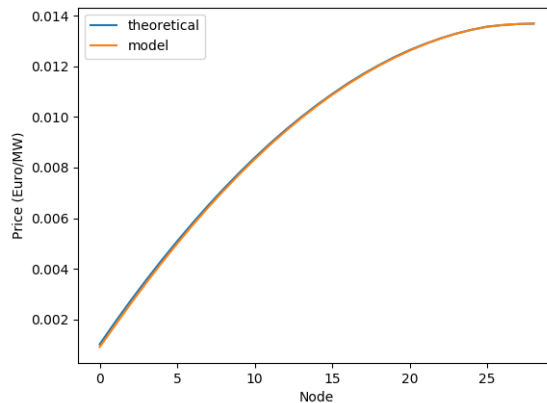


Figure A.3: Comparison between the evolution of the price along the line in theory and when the model is solved. This is the case of consumed power at each node.

